The Plant Cell, Vol. 18, 225–242, January 2006, www.plantcell.org

Polar Localizing Class V Myosin Chitin Synthases Are Essential during Early Plant Infection in the Plant Pathogenic Fungus *Ustilago maydis* [W]

Isabella Weber,[1] Daniela Aßmann, Eckhard Thines,[2] and Gero Steinberg[3]

Max-Planck-Institut für Terrestrische Mikrobiologie, D-35043 Marburg, Germany

Fungal chitin synthases (CHSs) form fibers of the cell wall and are crucial for substrate invasion and pathogenicity. Filamentous fungi contain up to 10 CHSs, which might reflect redundant functions or the complex biology of these fungi. Here, we investigate the complete repertoire of eight CHSs in the dimorphic plant pathogen *Ustilago maydis*. We demonstrate that all CHSs are expressed in yeast cells and hyphae. Green fluorescent protein (GFP) fusions to all CHSs localize to septa, whereas Chs5-GFP, Chs6-GFP, Chs7-yellow fluorescent protein (YFP), and Myosin chitin synthase1 (Mcs1)-YFP were found at growth regions of yeast-like cells and hyphae, indicating that they participate in tip growth. However, only the class IV CHS genes *chs7* and *chs5* are crucial for shaping yeast cells and hyphae ex planta. Although most CHS mutants were attenuated in plant pathogenicity, Δ*chs6*, Δ*chs7*, and Δ*mcs1* mutants were drastically reduced in virulence. Δ*mcs1* showed no morphological defects in hyphae, but Mcs1 became essential during invasion of the plant epidermis. Δ*mcs1* hyphae entered the plant but immediately lost growth polarity and formed large aggregates of spherical cells. Our data show that the polar class IV CHSs are essential for morphogenesis ex planta, whereas the class V myosin-CHS is essential during plant infection.

INTRODUCTION

Chitin, the β-(1→4)–linked polymer of *N*-acetylglucosamine, provides strength to the fungal cell wall and is therefore essential for the morphogenesis and survival of fungi (Ruiz-Herrera et al., 2002). The synthesis of chitin is mediated by membrane-bound chitin synthases (CHSs) that locate to specialized transport vesicles, the chitosomes (Bracker et al., 1976; Leal-Morales et al., 1994; Sietsma et al., 1996) or to the plasma membrane (Duran et al., 1979; Leal-Morales et al., 1988; Martinez and Gozalbo, 1994). The yeast *Saccharomyces cerevisiae* contains three CHSs that have cell cycle–specific functions in septum formation and during budding (Cabib et al., 2001). By contrast, the genome of filamentous fungi encodes up to 10 CHSs (Miyazaki and Ootaki, 1997) grouped in five classes, with class III and class V typical for filamentous fungi (Munro and Gow, 2001; Ruiz-Herrera et al., 2002). It was suggested that numerous CHSs cooperate in the fungal cell to support certain processes, such as septation and hyphal growth (Roncero, 2002). This model is based on the observation that mutants in single CHS genes of class I, class II, and class IV are often without obvious defects (Motoyama et al., 1994, 1996; Specht et al., 1996), whereas double mutants show mutant phenotypes (Motoyama et al., 1996; Fujiwara et al., 2000; Wang et al., 2001; Ichinomiya et al., 2002) or are not viable (Shaw et al., 1991). Alternatively, it is believed that filamentous fungi contain numerous CHSs to obtain a certain plasticity to explore different ecological niches and cope with their complex life cycle (Ruiz-Herrera et al., 2002). This concept is supported by the fact that certain CHSs are active during defined developmental stages of *Aspergillus nidulans* (Lee et al., 2004).

Pathogenic development of the maize (*Zea mays*) smut fungus *Ustilago maydis* is accompanied by numerous morphological transitions (Banuett and Herskowitz, 1996). In the yeast stage, haploid yeast-like cells grow by polar budding. Upon pheromone-dependent recognition, the fungus switches to hyphal tip growth and forms conjugation tubes that grow toward the mating partner. Subsequently, these cells fuse to build up a dikaryotic hypha that invades the plant tissue, where the fungus proliferates and causes the symptoms of maize smut disease. At present, six CHS genes have been reported in *U. maydis*, and null mutants in these were without significant phenotype (Gold and Kronstad, 1994; Xoconostle-Cazares et al., 1996, 1997), whereas mutants in the class V *chs6* were slightly thicker and showed reduced pathogenicity, indicating that this CHS is most important in *U. maydis* (Garcerá-Teruel et al., 2004). Here, we report the identification of two additional CHSs, *chs7*, a second class IV CHS gene, and *myosin chitin synthase1* (*mcs1*), another class V CHS with an N-terminal myosin motor domain in *U. maydis*. To further analyze the role of all CHSs in dimorphic switch, we obtained the published CHS null mutant strains (Δ*chs1* and a plasmid for the deletion of *chs2* obtained from J. Kronstad, and Δ*chs3* to Δ*chs6* kindly provided by J. Ruiz-Herrera). However, DNA gel

[1] Current address: Deutsches Krebsforschungszentrum, Im Neuenheimer Feld 280, D-69120 Heidelberg, Germany.
[2] Current address: Institut für Biotechnologie und Wirkstoff-Forschung, Erwin-Schrödinger-Strasse 56, D-67663 Kaiserslautern, Germany.
[3] To whom correspondence should be addressed. E-mail gero.steinberg@staff.uni-marburg.de; fax 49-6421-178-599.
The author responsible for distribution of materials integral to the findings presented in this article in accordance with the policy described in the Instructions for Authors (www.plantcell.org) is: Gero Steinberg (gero.steinberg@staff.uni-marburg.de).
[W] Online version contains Web-only data.
Article, publication date, and citation information can be found at www.plantcell.org/cgi/doi/10.1105/tpc.105.037341.

blot experiments and analytic PCR demonstrated that in the putative Δ*chs3*, Δ*chs4*, and Δ*chs5* strains, the corresponding gene was neither deleted nor disrupted. Therefore, we generated these strains and included them in our analysis.

Here, we describe an extensive analysis of the role of all eight CHSs in the morphogenesis of *U. maydis* yeast-like cells, pheromone-induced mating tubes, and dikaryotic hyphae. In addition, we generated yellow fluorescent protein/green fluorescent protein (YFP/GFP) fusion proteins and correlated their localization in yeast and hyphae with their importance in morphology and plant pathogenicity. We found that only Chs5, Chs6, Chs7, and Mcs1 localize to the growth region, which corresponds with essential functions of these CHSs in certain stages of the pathogenic development of *U. maydis*.

RESULTS

The Genome of *U. maydis* Encodes Eight CHSs

To identify additional CHS genes in *U. maydis*, we screened the recently published genome (see Methods for URL). This led to the identification of eight CHSs (Chs1 to Chs7 and Mcs1). Fragments of the sequences of *chs1* (accession number M82958) and *chs2* (accession number M82959) were published by Gold and Kronstad (1994). In addition, Xoconostle-Cazares et al. (1996, 1997) published the open reading frames of *chs3* (accession number X87748), *chs4* (accession number X87749), *chs5* (accession number AF030553), and *chs6* (accession number AF030554). However, we compared these sequences with the genomic sequence provided by Bayer CropScience and the Broad Institute (see Methods for URL). This analysis revealed major discrepancies for *chs4*, starting at base pair 1812. In addition, we determined the 3′ ends of all CHS genes (see Methods). This information, together with the sequence provided by the Broad Institute, led to new sequence predictions for the whole repertoire of CHSs in *U. maydis*, including the two new genes *mcs1* and *chs7* (Figure 1A). Comparison with other CHSs showed that Chs1 to Chs7 and Mcs1 belong to five classes (Figure 1A) (classification was done according to Munro and Gow [2001] and Mellado et al. [2003]). Chs3 and Chs4 group in class I and are 47% identical to each other, whereas Chs5 and Chs7 are 29% identical and belong to class IV. The sizes of the predicted proteins range from 880 amino acids for Chs2 to 2005 amino acids for Mcs1, which contains an N-terminal myosin-like domain that shows 22% sequence identity with the motor domain of Myo5, a myosin V from *U. maydis* (Weber et al., 2003) (Figure 1B). All CHSs contain a core region of 308 to 341 amino acids that is 15 to 64% identical to the defined conserved core region of ScChs2p from *Saccharomyces cerevisiae* (Nagahashi et al., 1995) (Figure 1B). In addition, each gene contains numerous putative transmembrane domains (Figure 1B).

The Class IV CHSs Chs5 and Chs7 Are Required for the Proper Morphology of Yeast-Like Cells

In axenic culture, *U. maydis* grows as a yeast-like cell that forms a polar bud. Upon initiation of pathogenic development, compatible cells switch to filamentous growth and form conjugation hyphae that fuse and give rise to a dikaryotic hypha, which enters the plant to complete the life cycle. To check whether CHSs are specifically expressed in yeast or hyphal cells, we isolated RNA from haploid yeast-like cells of wild-type strain FB2 and performed RNA gel blot analysis. We found that all CHSs were expressed at this stage (Figure 2A), suggesting that all of the corresponding gene products participate in wall formation of yeast-like cells. To obtain quantitative data on the expression level of CHS genes in *b*-dependent hyphae versus yeast-like cells, we performed real-time PCR. We found a transcriptional upregulation of *chs1* (~11.5-fold) and *chs4* (~13.5-fold) in hyphae of *U. maydis*, whereas no or only minor induction was found for the other CHS genes (Figure 2B). This could indicate that Chs1 and Chs4 are of particular importance for the filamentous growth of *U. maydis*. To gain further insights into the role of CHSs in *U. maydis*, we generated null mutants of *chs2*, *chs3*, *chs4*, *chs5*, *chs7*, and *mcs1* (see Methods; strain details are listed in Table 1). In addition, we included in our analysis the previously published mutant strains of *chs1* (Gold and Kronstad, 1994) and *chs6* (Garcerá-Teruel et al., 2004). None of these mutants showed impaired growth in axenic cultures, and doubling times ranged from 1.9 ± 0.04 h (Δ*chs4*) to 2.2 ± 0.06 h (Δ*chs2*); for control strain FB2, it was 2.1 ± 0.01 h. Consistently, most CHSs were of minor importance for the morphology of yeast-like cells (Figure 3A). Δ*chs1* cells were found to be slightly shorter, and Δ*chs6* and Δ*mcs1* mutant cells were significantly thicker than control cells of strain FB2 (Figure 3A). Only mutants in the class IV genes *chs5* and *chs7* exhibited drastic morphological defects in yeast-like cells. Δ*chs5* cells were elongated and had an irregular shape (Figure 3B, inset), with 11% of all cells showing a tendency to form cell chains (Figure 3B). By contrast, Δ*chs7* mutants displayed a cell separation defect, were slightly thicker, and occasionally lost the normal cell shape (Figure 3C). It was reported previously that Δ*chs5* mutants have no morphological defect, although the pathogenicity of these mutants was attenuated (Xoconostle-Cazares et al., 1997).

To gain further support for our findings, we confirmed the absence of the *chs5* mRNA in our Δ*chs5* mutant strains (Figure 3D). Moreover, we rescued the morphology defects of Δ*chs5* and also Δ*chs7* mutants (data not shown) with the wild-type copy of the gene on a self-replicating plasmid (Figure 3D; ΔChs5 + pCHS5), whereas the empty plasmid had no positive effect on the mutant phenotype (Figure 3D; ΔChs5 + empty plasmid). Finally, we obtained more direct indications for defects in chitin organization in Δ*chs5* and Δ*chs7* mutant cells by staining with rhodamine-conjugated wheat germ agglutinin, which specifically binds to *N*-acetylglucosamine (Nagata and Burger, 1974). Chitin was intensively stained in the growth region of control cells (Figure 3E, control, arrows) and at the bud scar (arrowhead), whereas lateral walls were only weakly stained. This staining pattern was found in most CHSs, suggesting that CHSs have overlapping functions in growth and septation. By contrast, in Δ*chs5* mutants no chitin cap was seen at growth regions and only patchy accumulations were detected (Figure 3E, ΔChs5, arrows). The lateral walls were significantly less fluorescent (Figure 3F), suggesting that the irregular shape of Δ*chs5* mutants is a consequence of defects in chitin incorporation. Δ*chs7* mutant cells also showed reduced chitin in the bud. However,

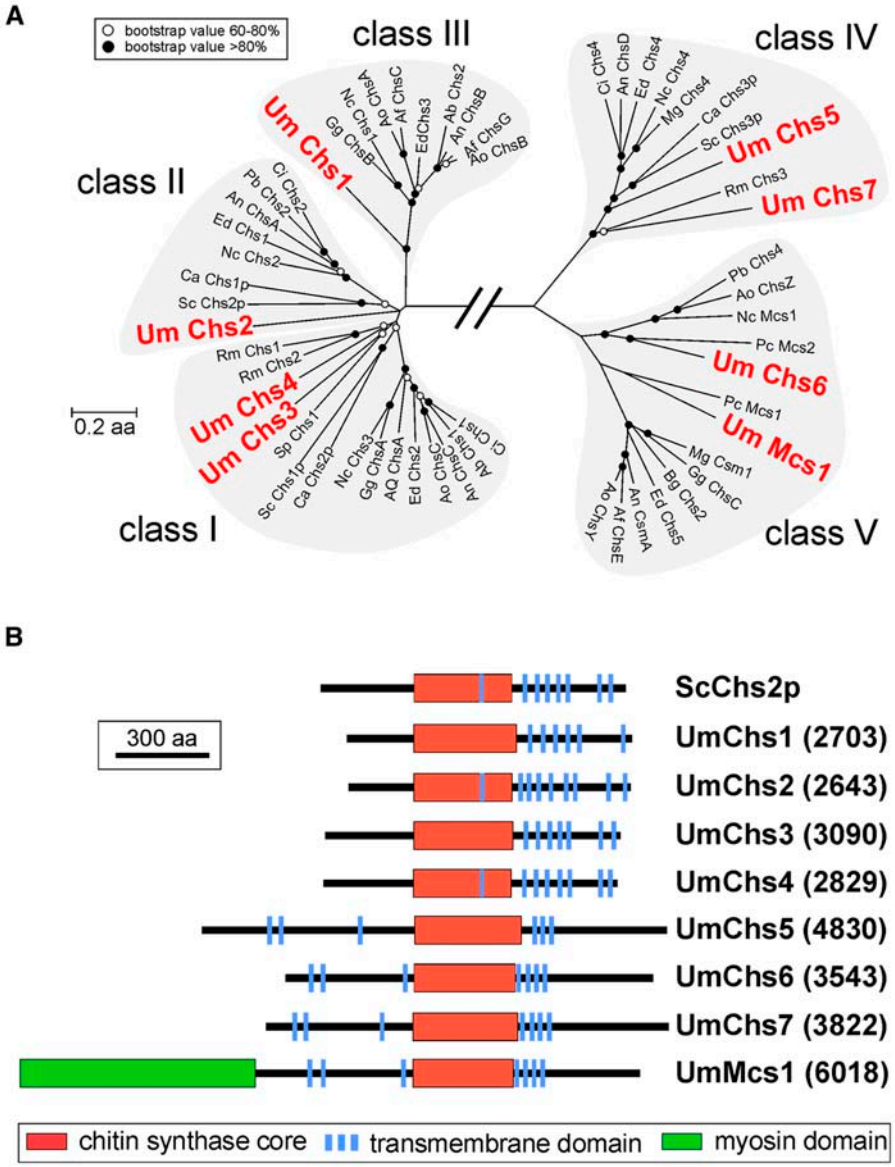

Figure 1. Sequences of CHSs in *U. maydis.*

(A) Comparison of the eight CHSs that were identified in the genomic sequence of *U. maydis* (see Methods for URL). Fragments of UmChs1 and UmChs2 were published by Bowen et al. (1992). Partial sequence information for UmChs3, UmChs4 UmChs5, and Umchs6 was reported previously (Xoconostle-Cazares et al., 1996, 1997). In addition, the *U. maydis* genome encodes a class IV CHS (Chs7, hypothetical protein UM05480; and the myosin-CHS Mcs1, hypothetical protein UM3204_1). Dendrograms are based on the complete amino acid sequence (see Supplemental Table 1 online for sequence alignment). Af, *Aspergillus fumigatus*; An, *Aspergillus nidulans*; Ao, *Aspergillus oryzae*; Aq, *Ampelomyces quisqualis*; Bg, *Blumeria graminis*; Ca, *Candida albicans*; Ci, *Coccidioides immitis*; Ed, *Exophiala dermatiditis*; Gg, *Glomerella graminicola*; Mg, *Magnaporthe grisea*; Nc, *Neurospora crassa*; Pb, *Paracoccioides brasiliensis*; Pc, *Phanerochaete crysosporium*; Rm, *Rhizopus microsporus*; Sc, *Saccharomyces cerevisiae*; Sp, *Schizosaccharomyces pombe.* Note that only the 3′ ends of all CHSs were experimentally determined; the start of all genes is predicted based on comparison with published CHS gene sequences from other species.

(B) Domain organization of the CHSs from *U. maydis.* The predicted gene products share 15 to 73% sequence identity in the central CHS core region containing parts that most likely provide the enzymatic activity. In addition, numerous transmembrane domains are predicted. Mcs1 contains an N-terminal domain that shows significant homology with the motor domain of myosins. The domain organization of Chs2p from *S. cerevisiae* is given for comparison. aa, amino acids.

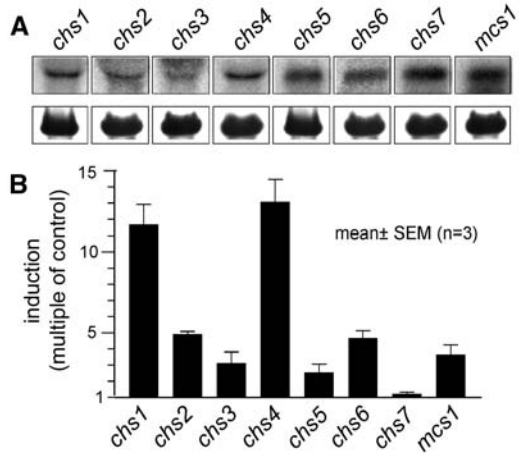

Figure 2. Expression Profile of CHS Null Mutants in Liquid Culture.

(A) RNA gel blot of RNA isolated from yeast-like cells of *U. maydis*. All CHS genes are expressed in sporidia.

(B) Quantitative real-time PCR revealed that *chs1* and *chs4* are transcriptionally upregulated in hyphae of *U. maydis* (strain AB33). Note that Δ*chs1* and Δ*chs4* mutant hyphae are without phenotype, whereas *chs7*, which is transcriptionally not induced, is of high importance for the filamentous growth of *U. maydis*. Values are given as means ± SE ($n = 3$).

compared with control cells, even stronger staining was detected in the mother cells (Figures 3F and 3G), suggesting that Chs7 participates in wall synthesis in the bud but also influences the composition of the lateral cell wall of the mother cell. In summary, these data indicate that Chs5 and Chs7 have important roles in wall formation and the morphology of yeast-like cells.

Nikkomycin Z Affects Tip Morphology in Yeast-Like Sporidia

Nikkomycin Z is a competitive inhibitor of CHSs (Gaughran et al., 1994), and we next analyzed the effect of this drug on our mutant strains. Surprisingly, treatment of wild-type cells with 5 μM Nikkomycin Z led to a swelling of the bud tip (Figure 4A, arrows), indicating that the inhibitor blocks the activity of polar CHSs at the growing end of the cell. Finally, cells formed large vacuoles and died from this treatment (Figure 4A, NZ, 2 h), suggesting that inhibition of CHSs blocked all growth, thereby arresting the cell cycle and killing the cells. Calcofluor staining revealed this polar swelling in large-budded cells that had formed a primary septum, suggesting that the cells continued polar cell wall synthesis during septum formation and cytokinesis in the G1 phase (Figure 4A, septum marked by an asterisk). We next determined a concentration of Nikkomycin Z at which wild-type cells were able to survive on plates but were impaired in growth (Figure 4B). At 1 μM Nikkomycin Z, no difference between wild-type strain FB2 and Δ*chs2*, Δ*chs3*, and Δ*chs4* cells was found. However, growth of Δ*chs1*, Δ*chs5*, Δ*chs6*, Δ*chs7*, and Δ*mcs1* was inhibited (Figure 4B). Considering our observation that Nikkomycin Z inhibits cell wall synthesis at the growing tip of the cell, these findings might indicate that the inhibited Chs1, Chs5 to Chs7, and Mcs1 participate in cell wall synthesis at the growing cell pole. However, Nikkomycin Z treatment in liquid culture also led to a slight increase in the swelling of mother cells in Δ*chs6* mutants (Figure 4C), and many dead Δ*chs6* mutant cells were found after 1 h of 5 μg/mL Nikkomycin Z incubation. Notably, wild-type cells were still viable in these conditions (Figure 4A). The reason for this high sensitivity of Δ*chs6* mutants to Nikkomycin Z is not known.

All CHSs Localize to the Septa of Yeast-Like Cells and Hyphae, whereas Chs5 to Chs7 and Mcs1 Are Also Found at the Growing Bud and Hyphal Tips

To gain further support for the notion that some CHSs are active at the growth region, we fused GFP or YFP to the 3′ ends of all CHS genes and integrated these constructs into the endogenous loci. Applying this strategy, we were able to visualize Chs3-GFP, Chs4-GFP, Chs5-GFP, Chs6-GFP, Chs7-YFP, and Mcs1-YFP, but we failed to detect Chs1-GFP and Chs2-GFP. Using anti-GFP antibodies, we were able to detect a band of the right size of Chs1-GFP in protein gel blots, but no Chs2-GFP was found, suggesting that the levels of Chs1-GFP were too low to be visualized, whereas Chs2-GFP might be expressed below the detection limits of protein gel blots.

Surprisingly, we found that GFP/YFP fusion proteins of all CHSs localized to the septa of yeast-like cells (Figures 5A and 5C), indicating that they all participate in septum formation. Only Chs5-GFP, Chs6-GFP, Chs7-YFP, and Mcs1-YFP localized to the growing bud tip (Figures 5A and 5B), and preliminary evidence from inhibitor studies suggests that their localization depends on the actin cytoskeleton (data not shown). The same distribution pattern was found in mating tubes (data not shown) and dikaryotic hyphae, where Chs5-GFP, Chs6-GFP, and Mcs1-YFP showed a tip-ward gradient (Figures 5D and 5E) or, in the case of Chs7-YFP, a distinct and pointed localization at the hyphal apex (Figure 5E). This local concentration of Chs7 suggests that its activity is restricted to the tip of the hypha, whereas the other CHSs might synthesize chitin within the whole hyphal apex. All CHSs localized to the basal septum that separates the living tip cell from the vacuolated part of the hypha (Figure 5F). These data clearly demonstrate that CHSs specifically localize to sites of exocytosis in yeast-like cells and hyphae, where they might cooperate to support septum formation or polar cell growth.

The Polar CHSs Chs5, Chs6, and Chs7 Are Important for Mating Tube and Dikaryotic Hyphae Formation

The pathogenic development of *U. maydis* is initiated by the recognition of the pheromone secreted by a mating partner. This results in cell cycle arrest and the formation of conjugation hyphae (Garcia-Muse et al., 2003). To investigate the role of CHSs in this important developmental stage, we made use of synthetic pheromone. Pheromone treatment of cells in liquid culture results in the formation of long conjugation hyphae (Szabo et al., 2002), and this allowed us to quantify tube formation in the CHS null mutant strains (Figure 6A). Our analysis revealed that only Δ*chs2* and Δ*mcs1* reacted normally to pheromone, whereas Δ*chs1*, Δ*chs3*, Δ*chs4*, and Δ*chs6* formed

Table 1. Strains and Plasmids Used in This Study

Strains/Plasmids	Genotype	Reference
FB1	*a1 b1*	Banuett and Herskowitz (1989)
FB2	*a2 b2*	Banuett and Herskowitz (1989)
FB6a	*a2 b1*	Banuett and Herskowitz (1989)
FB6b	*a1 b2*	Banuett and Herskowitz (1989)
SG200	*a1 mfa2 bW2 bE1*, ble^R	Bölker et al. (1995)
SG1	*a2 b2* Δ*chs1*, hyg^R	Gold and Kronstad (1994)
IW 248	*a2 b1* Δ*chs1*, hyg^R	This study
IW 249	*a1 b2* Δ*chs1*, hyg^R	This study
ΔChs2	*a2 b2* Δ*ch2*, ble^R	This study
IW 253	*a1 b2* Δ*chs2*, ble^R	This study
IW 254	*a2 b1* Δ*chs2*, ble^R	This study
ΔChs3	*a2 b2* Δ*chs3*::ble^R	This study
IW 102	*a1 b2* Δ*chs3*::ble^R	This study
IW 101	*a2 b1* Δ*chs3*::ble^R	This study
ΔChs4	*a2 b2* Δ*chs4*::hyg^R	This study
IW 84	*a2 b2* Δ*chs4*::hyg^R	This study
IW 85	*a1 b1* Δ*chs4*::hyg^R	This study
ΔChs5	*a2 b2* Δ*chs5*::ble^R	This study
IW 89	*a1 b1* Δ*chs5*::ble^R	This study
SG200ΔChs5	*a1 mfa2 bW2 bE1* Δ*chs5*::hyg^R	This study
FB1ΔChs6	*a1 b1* Δ*chs6*, hyg^R	Garcerá-Teruel et al. (2004)
AG2	*a2 b2* Δ*chs6*, hyg^R	Garcerá-Teruel et al. (2004)
SG200ΔChs6	*a1 mfa2 bW2 bE1* Δ*chs6*::hyg^R	This study
FB1ΔChs7	*a1 b1* Δ*chs7*::hyg^R	This study
FB2ΔChs7	*a2 b2* Δ*chs7*::hyg^R	This study
SG200ΔChs7	*a1 mfa2 bW2 bE1* Δ*chs7*::hyg^R	This study
FB1ΔMcs1	*a1 b1* Δ*mcs1*::hyg^R	This study
FB2ΔMcs1	*a2 b2* Δ*mcs1*::hyg^R	This study
FB1ΔChs6ΔMcs1	*a1 b1* Δ*chs6*, hyg^R Δ*mcs1*::ble^R	This study
IW46	*a2 b2* Δ*chs6*, hyg^R Δ*mcs1*::ble^R	This study
SG200ΔMcs1	*a1 mfa2 bW2 bE1* Δ*mcs1*::hyg^R	This study
SG200ΔMcs1OGMcs1	*a1 mfa2 bW2 bE1* Δ*mcs1*::hyg^R/*pOGMcs1*	This study
FB2ΔChs7pChs7	*a2 b2* Δ*chs7*::hyg^R + *pChs7*	This study
FB1ΔChs7pChs7	*a1 b1* Δ*chs7*::hyg^R + *pChs7*	This study
FB1ΔChs7pNEBUC	*a1 b1* Δ*chs7*::hyg^R + *pNEBUC*	This study
FB2ΔChs7pNEBUC	*a2 b2* Δ*chs7*::hyg^R + *pNEBUC*	This study
FB2ΔChs5pChs5	*a2 b2* Δ*chs5*::ble^R + *pChs5*	This study
FB2ΔChs5pNEBUH	*a2 b2* Δ*chs5*::ble^R + *pNEBUH*	This study
FB2Chs1GFP	*a2 b2 chs1-gfp*, ble^R	This study
FB2Chs2GFP	*a2 b2 chs2-gfp*, ble^R	This study
FB2Chs3GFP	*a2 b2 chs3-gfp*, ble^R	This study
FB2Chs4GFP	*a2 b2 chs4-gfp*, ble^R	This study
FB2Chs5GFP	*a2 b2 chs5-gfp*, ble^R	This study
FB2Chs6GFP	*a2 b2 chs6-gfp*, ble^R	This study
FB2Chs7YFP	*a2 b2 chs7-yfp*, hyg^R	This study
AB33Chs7YFP	*a2 b2 Pnar1:bW2*, *bE1 pchs7-yfp*, hyg^R	This study
FB2Mcs1YFP	*a2 b2 mcs1-yfp*, hyg^R	This study
AB33Mcs1YFP	*a2 b2 Pnar1:bW2*, *bE1pmcs1-yfp*, hyg^R	This study
FB2ΔAdr1	*a2 b2* Δ*adr1*::nat^R	This study
FB2ΔAdr1ΔMcs1	*a2 b2* Δ*adr1*::nat^RΔ*mcs1*::hyg^R	This study
pOGMcs1	*Potef-egfp-mcs1*, cbx^R	This study
pChs5	*Pchs5-chs5-Tchs5*, hyg^R, *Uars*	This study
pChs7	*Pchs7-chs7-Tchs7*, cbx^R, *Uars*	This study
pNEBUC	cbx^R, *Uars*	Weinzierl (2001)
pNEBUH	hyg^R, *Uars*	Weinzierl (2001)

a, *b*, mating-type loci; Δ, deletion; *P*, promoter; ::, homologous replacement; -, fusion; +, free-replicating plasmid; hyg^R, hygromycin resistance; ble^R, bleomycin resistance; cbx^R, carboxin resistance; nat^R, nourseothricin resistance; /, ectopically integrated; *E1*, *W2*, genes within the *b* mating-type locus; *egfp*, enhanced green fluorescent protein; *yfp*, yellow fluorescent protein; *T*, terminator; Uars, *U. maydis* autonomously replicating sequence.

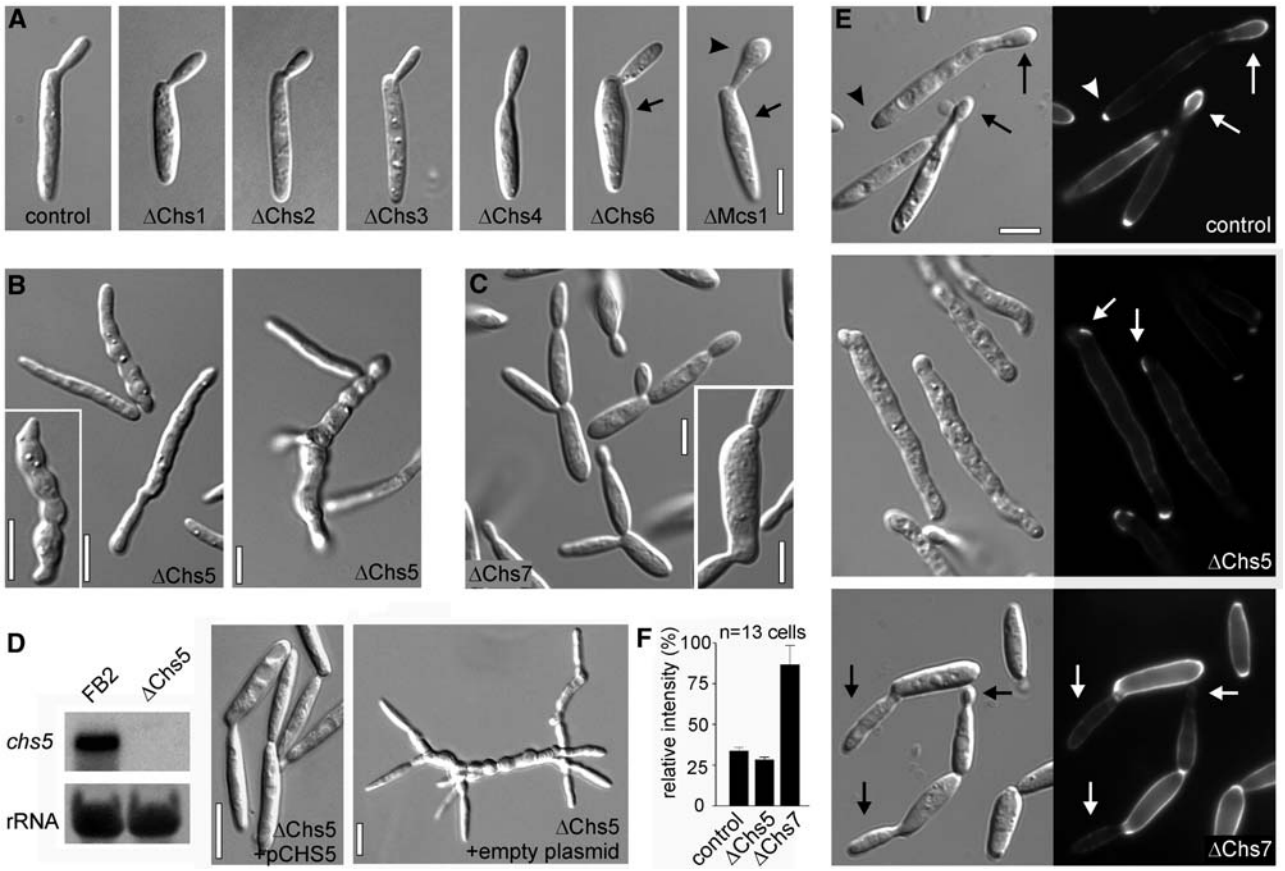

Figure 3. Morphology of Yeast-Like CHS Null Mutants.

(A) The deletion of most CHSs had no or only minor effects on the shape of haploid yeast-like cells. Δ*chs6* mutant mother cells were thicker (arrow), and a small portion of Δ*mcs1* cells showed swelling of the bud tip and, occasionally, also of the mother cell. Bar = 5 μm.

(B) Δ*chs5* mutants grow irregularly (see inset) and often lose the neck constriction that separates the mother and the daughter cells. Furthermore, ~11% of all cells formed cell chains, indicating that the activity of Chs5 is essential for the proper morphology of yeast-like cells. Bars = 5 μm.

(C) Deletion of the newly identified *chs7* led to a significant swelling of mother cells (see inset) and resulted in a cell separation defect. Bars = 5 μm.

(D) The phenotype of Δ*chs5* mutants was in contradiction to previous reports (Xoconostle-Cazares et al., 1997). However, RNA gel blot analysis confirmed the absence of the *chs5* message in deletion strains. Moreover, the morphology phenotype could be rescued by expression of Chs5 from a self-replicating plasmid (ΔChs5 + pCHS5), whereas the empty plasmid (ΔChs5 + empty plasmid) was without effect. Bars = 5 μm.

(E) Chitin staining with rhodamine-conjugated wheat germ agglutinin demonstrates that chitin is deposited at the growing bud (control, arrows). In addition, the bud scar is detected (control, arrowhead). In Δ*chs5* mutants, chitin staining is strongly reduced and no buds are detected (ΔChs5). Instead, chitin accumulates in patches at the cell poles (ΔChs5, arrows). Surprisingly, Δ*chs7* mutants had almost no chitin staining in the growing buds (ΔChs7, arrows) but an unusually strong staining of the mother cell wall. This indicates that the absence of this CHS leads to defects in chitin depositioning or maturation of the cell wall. Bar = 5 μm.

(F) Quantitative analysis of the rhodamine wheat germ agglutinin signal intensity in the lateral cell wall demonstrates that deletion of *chs5* reduced the chitin content (ΔChs5), whereas deletion of Chs7 increased the wheat germ agglutinin signal (ΔChs7). Values are given as means ± SE (n = 12 to 18).

significantly fewer tubes (Figure 6A). Both Chs5 and Chs7 activity was essential for tube formation, as mutants in both CHSs were strongly impaired in the formation of conjugation hyphae (Figure 6A). This finding suggests that Chs5 and Chs7 have a role in the initial polar growth of tubes. However, at present, we cannot exclude the unlikely possibility that both CHSs participate in pheromone sensing, which would lead to a similar phenotype. In both mutants, a small number of tubes were still formed. Although these looked almost normal in Δ*chs5* strains (Figure 6B), Δ*chs7* mutants formed only very thick and irregular extensions (Figure 6B), indicating that Chs7 is needed not only for the formation but also for the morphology of conjugation hyphae.

Mating tube growth is followed by cell fusion and the formation of a dikaryotic hypha. This reaction can be visualized on charcoal-containing plates (Holliday, 1974), where haploid yeast-like cells appear grayish, whereas successful mating leads to the formation of a white and fuzzy colony consisting of dikaryotic hyphae (Figure 6C, control; compatible partners are

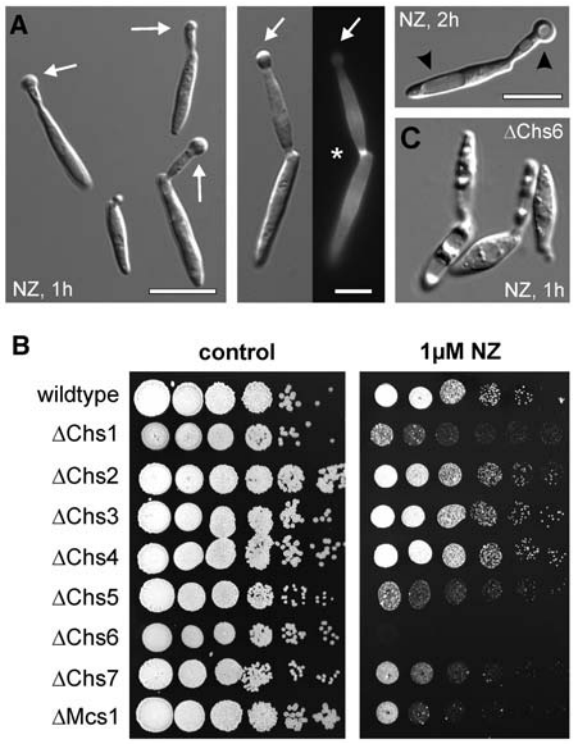

Figure 4. Effect of the CHS Inhibitor Nikkomycin Z on Wild-Type and CHS Null Mutant Strains.

(A) Incubation of growing cells with 5 μM Nikkomycin Z (NZ), a specific inhibitor of CHS, for 1 h leads to a swelling of the growing tip of the cell (arrows). Interestingly, this effect was also seen in large-budded cells that form septa, as indicated by Calcofluor staining (asterisk). After longer periods of drug treatment, cells formed large vacuoles (arrowheads) and died. Note that these cells did not burst, even when transferred into water, indicating that Nikkomycin Z–mediated inhibition of CHS at the growing cell pole only partially weakened the cell wall. Bars = 10 μm.

(B) Plate growth of wild-type cells was only slightly inhibited at 1 μM Nikkomycin Z. However, at this concentration, growth of Δ*chs1*, Δ*chs5*, Δ*chs7*, and Δ*mcs1* cells was impaired, whereas Δ*chs6* mutants did not form any colonies. Because Nikkomycin Z leads to swelling of the tip (see above), the hypersensitivity of Δ*chs1*, Δ*chs5*, Δ*chs6*, Δ*chs7*, and Δ*mcs1* mutants might reflect activity of these CHSs at the growth region.

(C) Incubation of Δ*chs6* mutants in 5 μg/mL Nikkomycin Z killed most cells and led to slight swelling of the mother cells. Note that control cells were still viable under these conditions.

indicated by a1b1 and a2b2, and the fuzzy colony is indicated by a1b1 × a2b2). The ability to form dikaryotic hyphae was tested by crossing compatible CHS null mutant strains on charcoal plates (Figure 6C). Impaired formation of a fuzzy colony was observed for Δ*chs5* × Δ*chs5*, Δ*chs7* × Δ*chs7*, and, to a minor extent, for Δ*chs6* × Δ*chs6* (Figure 6C). However, dikaryotic hyphae formation requires the fusion of conjugation tubes; therefore, we considered it possible that this phenotype is a secondary consequence of the described defect in conjugation hyphae formation of Δ*chs5*, Δ*chs6*, and Δ*chs7*. To circumvent the need for cell fusion, we generated the respective mutations in the solopathogenic strain SG200 (Bölker et al., 1995). Because of autocrine pheromone stimulation as well as the presence of an active bE/bW heterodimer, a transcription factor that controls filamentous growth and pathogenicity (reviewed in Feldbrügge et al., 2004), SG200 is able to form dikaryotic hyphae without a mating partner (Figure 6C, bottom row). Filament formation of SG200ΔChs5 and SG200ΔChs7 was attenuated after 24 h (Figure 6C, bottom row, ΔChs5 and ΔChs7), which strongly indicated that both CHSs have important additional roles in growth after cell fusion. After 2 d on charcoal, Δ*chs5* mutants recovered and formed hyphae that showed normal morphology (Figure 6D; see control for comparison). By contrast, neither compatible Δ*chs7* mutants nor SG200ΔChs7 strains formed a fuzzy colony, and short and irregular hyphae were rarely found (Figure 6E). These Δ*chs7* hyphae form empty sections (Figure 6E, SG200ΔChs7) but were thicker and much shorter, indicating that Chs7 is required for proper hyphal growth. These data demonstrate that Chs5 and Chs7 are critical for efficient conjugation tube formation, but only Chs7 appears to be crucial for filamentous hyphal growth.

The Myosin-CHS Is Not Required for Hyphal Morphology ex Planta

In other fungal systems, the deletion of Mcs1-like myosin-CHSs leads to defects in hyphal morphology (Horiuchi et al., 1999). Surprisingly, SG200ΔMcs1 hyphae were without any significant phenotype (Figures 6C and 6E), although it was expressed in the hyphal stage (Figure 2B) and localized to the growth region (Figure 5D). In contrast with other fungi, *U. maydis* encodes a second class V CHS, Chs6 (Xoconostle-Cazares et al., 1997); therefore, we assumed that both class V enzymes substitute for each other. Consequently, we generated a Δ*mcs1* Δ*chs6* double mutant and checked its morphology. Although single mutant yeast-like cells occasionally showed only minor defects (Figure 6F, ΔMcs1, arrow), the double mutant was much more swollen, which was most likely attributable to a weakening of the lateral cell walls (Figure 6F, ΔMcs1ΔChs6). Indeed, we were able to almost completely restore the mutant phenotype with 500 mM sorbitol (data not shown). By contrast, dikaryotic double mutant hyphae did not show any obvious defect (Figure 6G), indicating that class V CHSs are not essential for the proper hyphal growth of *U. maydis*.

Dikaryotic and SG200-derived hyphae are cell cycle arrested in G2 phase (Garcia-Muse et al., 2003) and consist of a single tip cell that leaves vacuolated sections behind (Steinberg et al., 1998). Thus, we considered it possible that Mcs1, although expressed in hyphae, is not active in these G2-arrested cells and therefore no phenotype is observed. Consequently, a hypha that is not cell cycle arrested could show the expected morphological phenotype. To test this possibility, we deleted *adr1*, a catalytic subunit of cAMP-dependent protein kinase (Dürrenberger et al., 1998) in the wild type and the Δ*mcs1* mutant background. Deletion of *adr1* leads to continuous hyphal growth without an arrest in the cell cycle (Dürrenberger et al., 1998). Indeed, strains FB2ΔAdr1 and FB2ΔAdr1ΔMcs1 formed long hyphae that consisted of numerous cellular compartments with individual nuclei (Figures 7A and 7B, arrowheads). Occasionally, we observed highly condensed and closely spaced nuclei, suggesting that

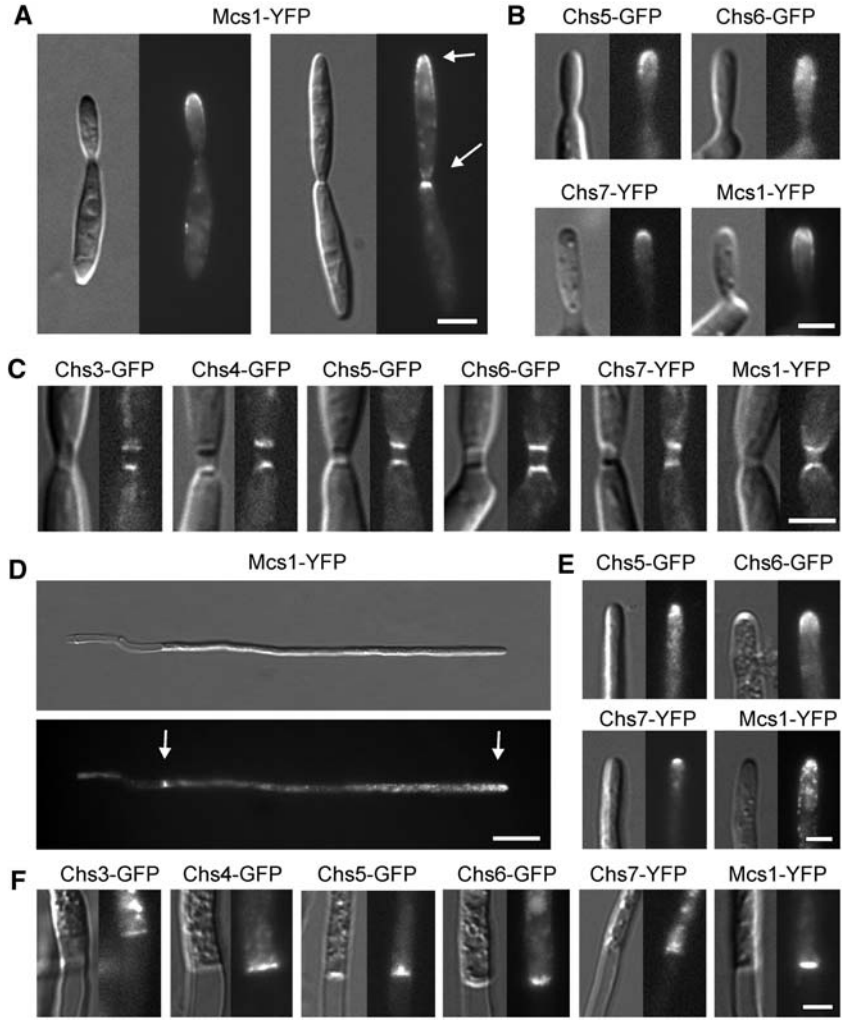

Figure 5. Localization of CHS-GFP/YFP Fusion Proteins in Haploid Yeast-Like Cells and Dikaryotic Hyphae.

(A) GFP or YFP fused to the 3′ end of endogenous CHS genes resulted in fluorescent fusion proteins that localized to septa and in some cases the growing tip of the bud (Msc1-YFP is given as an example). In large-budded cells, fusion protein was detected at the primary septum as well as at the bud tip (arrows), indicating that the cell still expands while it forms septa, a result that was also indicated by the Nikkomycin Z experiments (see Figure 4A). Bar = 3 μm.
(B) Fluorescent fusion proteins of Chs5, Chs6, Chs7, and Mcs1 localize to the growing bud. Note that Chs7-YFP forms a distinct point at the tip, whereas the other CHSs cover a broader region of the apex. Bar = 3 μm.
(C) All CHSs localize to secondary septa. Note that no signal was seen for Chs1-GFP, although small amounts were detected in protein gel blots (data not shown). Chs2-GFP was not detected on protein gel blots or by microscopy. Bar = 3 μm.
(D) In dikaryotic hyphae, most CHSs localized to the growing tip and septum that separates the living tip cell from the vacuolated older part of the hyphae (Mcs1-YFP is given as an example). Arrows mark the poles of the growing tip cell. Bar = 10 μm.
(E) Fluorescent fusion proteins of Chs5, Chs6, Chs7, and Mcs1 localize to the hyphal apex. Again, Chs7-YFP shows a very pointed localization. Bar = 3 μm.
(F) Similar to the situation in yeast-like cells, all CHS-GFP/YFP fusion proteins are found at the septa. Note that the CHS-GFP/YFP fusion proteins were functional, as they restored the phenotype of Δ*mcs1* mutants (see also Figure 7D) or did not cause the typical phenotypes when introduced into the endogenous locus of *chs5*, *chs6*, and *chs7*. Bar = 3 μm.

these cells are in mitosis (Figure 7A, asterisks). Consistent with the observations in the cell cycle–arrested *b*-dependent hyphae, deletion of *mcs1* had no significant effect on the morphology of these nonarrested hyphae, although some hyphae grew slightly irregularly (Figure 7B, bottom panel). Thus, we conclude that the absence of a clear mutant phenotype in Δ*mcs1* dikaryotic hyphae is not the result of a cell cycle–dependent regulation of the activity of Mcs1.

Finally, we checked whether Δ*mcs1* hyphae show alterations in the distribution of chitin in their cell wall. Treatment of control hyphae with 0.2 μg/mL rhodamine-conjugated wheat germ agglutinin for 10 min weakly labeled the lateral cell walls but

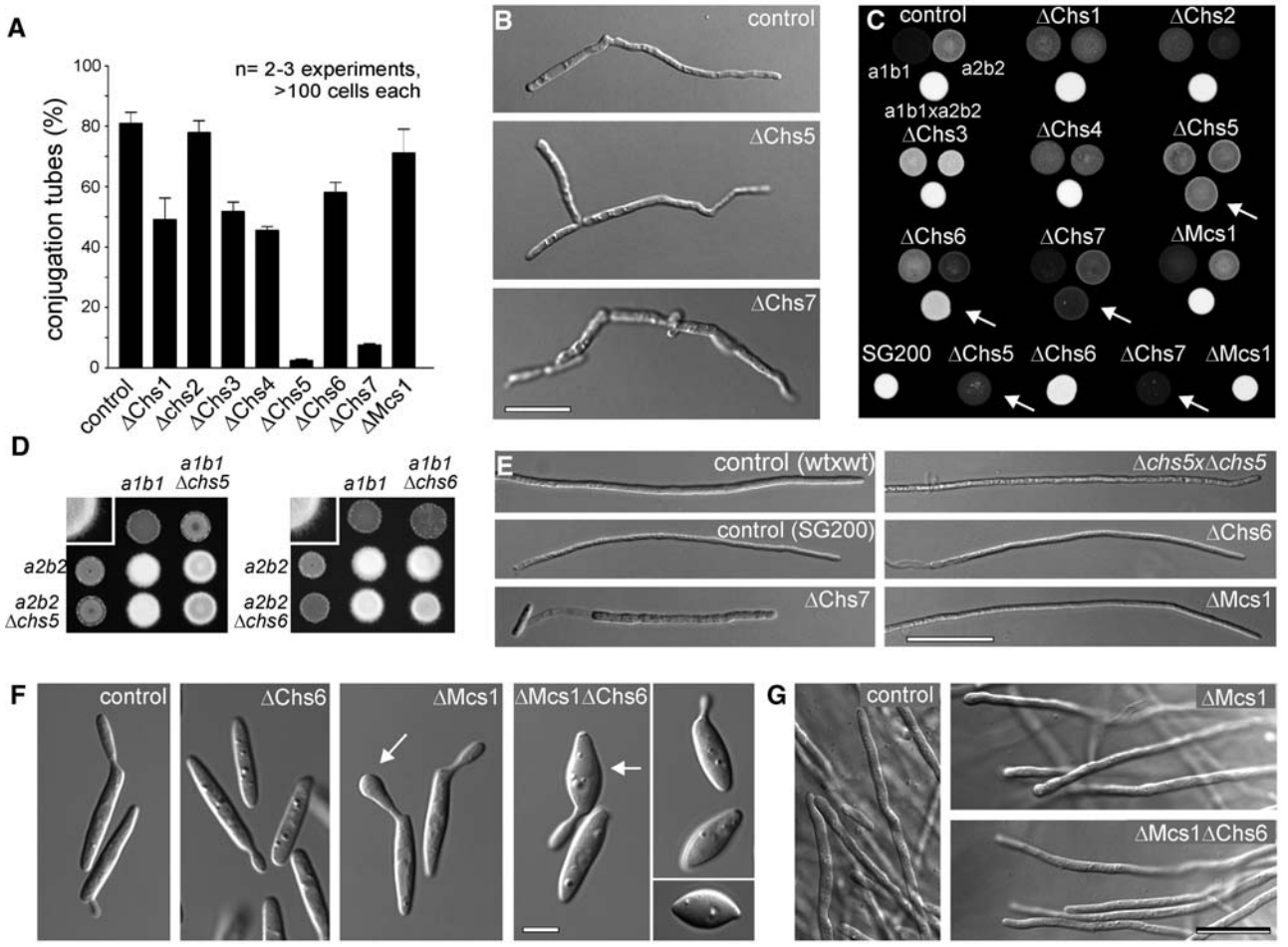

Figure 6. The Role of CHS in the Formation and Morphology of Conjugation and Dikaryotic Hyphae.

(A) In medium supplemented with synthetic pheromone, ~80% of wild-type cells form long conjugation hyphae (see [B], control). Under the same conditions, Δ*chs1*, Δ*chs3*, Δ*chs4*, and Δ*chs6* mutants showed significantly fewer hyphae, whereas the activity of Chs5 and Chs7 is crucial for tube formation. Values are means ± SE ($n = 2$ to 3 experiments, and at least 100 cells per experiment were analyzed).

(B) After 11 h of pheromone treatment, some Δ*chs5* conjugation hyphae were found that showed almost normal morphology. By contrast, Δ*chs7* mating tubes grew irregularly, had additional septa, and were much thicker. Bar = 10 μm.

(C) Crossing of compatible strains on charcoal-containing plates resulted in the formation of a fuzzy colony that is covered by white aerial hyphae (the genotype of control strains is indicated as an example). The formation of these filaments was attenuated in Δ*chs5* and Δ*chs6* strains and completely abolished in crossings of compatible Δ*chs7* mutants (arrows). Solopathogenic SG200 mutants form filaments without fusion to a mating partner, which results in a white colony (bottom row). However, SG200ΔChs5 and SG200ΔChs7 still did not form hyphae, indicating that both CHSs are important for hyphal growth.

(D) After 2 d on charcoal, compatible Δ*chs5* and Δ*chs6* strains form fuzzy colonies, indicating that filament formation is delayed in these mutants. Note that Δ*chs6* × Δ*chs6* colonies did not become white and fuzzy. Insets show larger magnifications of the colony edge.

(E) Control hyphae of crossings of compatible wild-type strains (*a1b1* × *a2b2*) and solopathogenic SG200 are indistinguishable from Δ*chs5* (Δ*chs5* × Δ*chs5*), Δ*chs6* (SG200ΔChs6), and Δ*mcs1* (SG200ΔMcs1) mutant hyphae. Only Δ*chs7* mutants show severely altered morphology (SG200ΔChs7). Bar = 30 μm.

(F) Deletion of *mcs1* and *chs6* led to minor defects in the morphology of yeast-like cells. Occasionally in Δ*mcs1*, the growing bud was swollen (ΔMcs1, arrow) and the mother cells were slightly thicker. By contrast, deleting both class V CHSs led to more drastic swellings of the Δ*mcs1* Δ*chs6* mutants (ΔMcs1ΔChs6, arrow). Note that this mutant phenotype varied between experiments and that extreme examples are shown. Bar = 3 μm.

(G) In contrast with yeast-like cells, deletion of *mcs1* and *chs6* did not affect the morphology of dikaryotic hyphae, indicating that both class V CHSs have minor roles in hyphal growth ex planta. Bar = 10 μm.

brightly stained the hyphal apex (Figure 7C, SG200, arrows). Line-scan analysis of the fluorescence intensity along the apical 30 μm confirmed the existence of the apical chitin cap in control hyphae (Figure 7D, SG200, arrow). Chitin staining of Δ*mcs1* hyphae was reduced slightly (Figures 7C and 7D, SG200ΔMcs1). Most strikingly, a prominent apical chitin cap was never found in mutant hyphae, suggesting that Mcs1 participates in chitin synthesis at the hyphal apex. However, this activity is not essential to maintain hyphal growth and morphology.

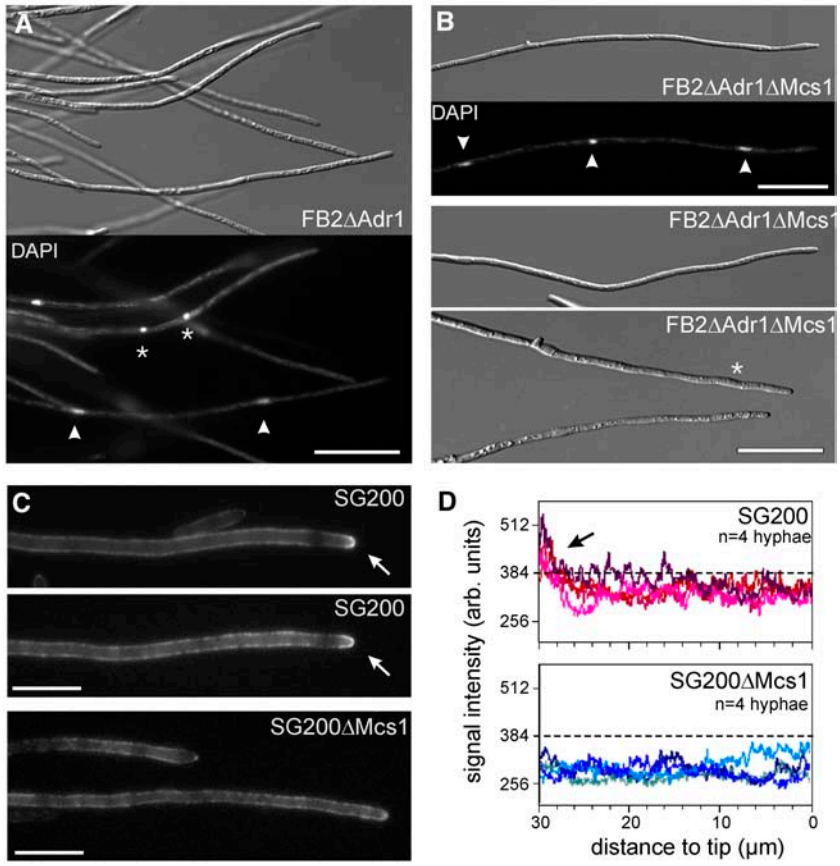

Figure 7. Δ*mcs1* Mutant Phenotype of cAMP-Dependent Filaments and Chitin Distribution in *b*-Dependent Hyphae.

(A) Deletion of *adr1*, which encodes the catalytic subunit of cAMP-dependent kinase (Dürrenberger et al., 1998), results in continuous filamentous growth of the haploid cells. Staining of nuclei with 4′,6-diamidino-2-phenylindole reveals that these hyphae contain numerous nuclei (arrowheads). Occasionally, condensed and closely spaced nuclei are seen (asterisks) that are indicative of a mitotic event, which demonstrates that cAMP-dependent hyphae are not cell cycle arrested. Bar = 20 μm.

(B) Δ*mcs1* Δ*adr1* double mutants also form multinucleated hyphae (nuclei indicated by arrowheads). Hyphal morphology is almost normal, although some hyphae appear thicker and less regular (asterisk). Thus, Mcs1 is dispensable for hyphal growth of continuously growing cAMP hyphae. Bars = 20 μm.

(C) Staining of chitin with low amounts of rhodamine-conjugated wheat germ agglutinin weakly labeled the lateral cell walls and a prominent chitin cap at the hyphal apex (SG200, arrows). Note that this chitin cap corresponds well with the localization of Mcs1 (see Figure 6). By contrast, this polar chitin cap is absent from Δ*mcs1* hyphae (SG200ΔMcs1). Bars = 10 μm.

(D) Quantitative line-scan analysis of the intensity of rhodamine-conjugated wheat germ agglutinin along the apical 30 μm of control (SG200) and Δ*mcs1* (SG200ΔMcs1) hyphae demonstrates that the amount of chitin in the lateral cell wall is reduced and that the apical chitin cap (arrow in top graph) is missing from mutant hyphae. These data suggest that Mcs1 participates in wall synthesis of *U. maydis* hyphae but that its activity is not crucial for hyphal morphology.

The Polar CHSs Chs6, Chs7, and Mcs1 Are Essential for Pathogenicity

Under natural conditions, mating and the formation of dikaryotic hyphae occur on the surface of the plant epidermis. To complete the pathogenic phase, *U. maydis* hyphae invade the plant tissue and undergo numerous developmental steps, including hyphae proliferation, fragmentation, and spore formation (Feldbrügge et al., 2004). The infection alternates plant growth, induces tumor formation, and eventually leads to the death of the plant (Figure 8A). To investigate the need for CHSs during pathogenic development, we infected maize seedlings and counted plants that had formed tumors ~14 d after infection. Surprisingly, these experiments revealed that most CHSs, including Chs5, were attenuated in pathogenic development (Figure 8C), which was best illustrated by the reduced average fresh weight of tumors induced by CHS mutants (Figures 8B and 8E). Moreover, Chs6, Chs7, and Mcs1 were found to be crucial for the formation of tumors (Figures 8A and 8C). The results obtained for Chs6 confirm previous reports on a pathogenicity defect of Δ*chs6* mutants (Garcerá-Teruel et al., 2004). The solopathogenic strain SG200ΔChs7 showed increased pathogenicity compared with the crossing of compatible Δ*chs7* mutant strains (Figure 8D), indicating that the observed conjugation tube formation defect of Δ*chs7* is a major cause of the reduced virulence of the mutants. However, in the absence of Chs7, mutant hyphae were

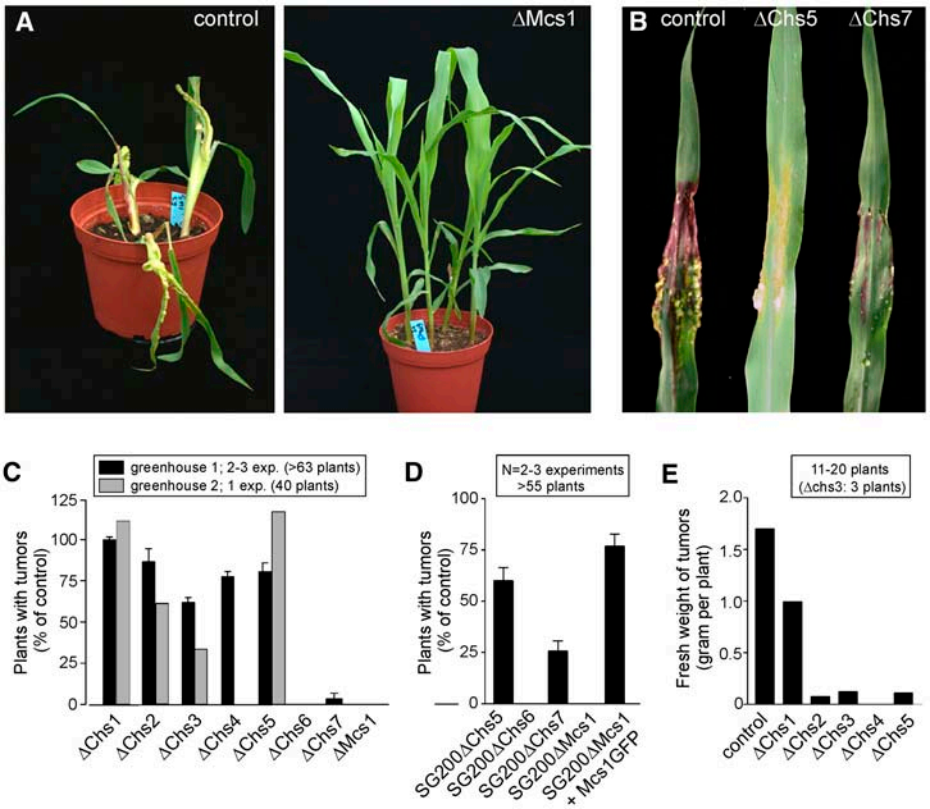

Figure 8. Pathogenicity of CHS Null Mutants.

(A) Infection of maize plants with compatible control or CHS mutant strains led to tumor formation in most inoculated plants and eventually killed the host. By contrast, compatible Δ*mcs1* mutant strains showed no symptoms, indicating that the deleted CHS is of great importance for plant infection.
(B) The solopathogenic strain SG200ΔChs5 showed ~60% of the virulence of control strains, and SG200ΔChs7 was able to infect ~30% of all plants. However, in both mutants, the resulting tumors were much smaller than those of control plants.
(C) Quantitative analysis of at least two experiments counting infected plants that formed tumors 14 to 16 d after infection revealed that Chs1 to Chs4 activity was of no or minor importance for plant infection (black bars), whereas Δ*chs6*, Δ*chs7*, and Δ*mcs1* were nonpathogenic (black bars). Values are given as means ± SE ($n = 2$ to 3 experiments and >63 plants). Under improved plant growth conditions, the virulence of control strains was attenuated (data not shown) and Δ*chs4* mutants also did not induce tumor formation (gray bars).
(D) In the solopathognic strain SG200ΔChs7, virulence was partially restored, indicating that the mating defect of Δ*chs7* mutants is largely responsible for the reduced pathogenicity, Values are given as means ± SE ($n = 2$ to 3 experiments and >55 plants). However, pathogenicity was at 25.7%, which argues for important roles of Chs7 in planta. SG200ΔMcs1 was still nonpathogenic, and virulence was restored by expression of a Mcs1-GFP fusion protein.
(E) Fourteen days after infection, tumors of plants infected with control cells and Δ*chs1* to Δ*chs5* were harvested and their fresh weight per plant was determined. Although CHS mutants formed tumors, the size of these tumors was drastically reduced, suggesting that all CHSs participate in pathogenic development.

still attenuated in virulence, and the observed tumors, induced by Δ*chs7* mutants, were significantly smaller than those of control plants, demonstrating that Chs7 is required for full virulence (Figure 8B).

In a second round of experiments, we made use of a newly built greenhouse that provided optimal conditions for the host plants. Under these improved environmental conditions, tumors appeared 5 to 6 d after infection in control and all CHS mutant strains tested, but only ~45% of all plants infected with wild-type cells developed tumors (normal rates are 70 to 90%), suggesting that the plants were less susceptible to the infection. Consequently, the damage caused by mutants in CHSs was also reduced. However, compared with the control, Δ*chs2* and Δ*chs3* were even less successful in these assays (Figure 8C, gray bars), and Δ*chs4* did not induce any tumors (Figure 8C, gray bars). Moreover, tumors were much smaller, as illustrated by the average fresh weight per infected plant (Figure 8E). These data demonstrate that the polar CHSs (Chs6, Chs7, and Mcs1) are essential for fungal virulence under various conditions, whereas Chs2, Chs3, and Chs4 become essential only under growth conditions that support the plant and that lead to reduced susceptibility to infections.

Δ*mcs1* Mutants Fail to Invade the Plant Epidermis

We found that Δ*mcs1* and Δ*chs6* mutants are nonpathogenic, indicating that class V CHSs play a crucial role in plant infection.

It has been described that Δ*chs6* mutants failed to colonize the plant tissue, which might be attributable to a defect in the early steps of infection (Garcerá-Teruel et al., 2004). To learn more about the pathogenicity defect of Δ*mcs1* mutants, we investigated the initial infection steps on fixed and KOH-cleared plant material, in which the fungus was visualized by chlorazole black staining (Brundett et al., 1996; Brachmann et al., 2003). Analysis of *Z* axis stacks revealed that 1 d after infection, control hyphae enter the plant epidermis without major morphological changes (Figure 9A, control; the depth of the optical plane is indicated in the bottom left corner). By contrast, even after 3 d, Δ*mcs1* hyphae reached only into the upper epidermal layer, where they formed large swellings (Figure 9A, ΔMcs1) that were approximately four times thicker than control hyphae (Figures 9C [arrowheads indicate the wall of a mesophyll cell] and 9D). These swellings are found inside the plant epidermis (Figures 9A [−10 μm] and 9B), whereas more straight hyphae were found on the plant surface (Figure 9A, 0 μm), suggesting that Δ*mcs1* hyphae lost the ability to grow in a directed manner after they entered the host epidermis. Instead, invading hyphae became apolar, indicating that Mcs1 is crucial for hyphal growth inside the plant. It was found recently that mutants in Mcs1-like CHSs of *Fusarium oxysporum* failed to invade tomato (*Lycopersicon esculentum*) plants because of a hypersensitivity to H_2O_2 (Madrid et al., 2003). Therefore, we checked our Δ*mcs1* and Δ*mcs1* Δ*chs6* strains on CM-G (for complete medium supplemented with 1% glucose) plates supplemented with low amounts of H_2O_2. Both the wild type and Δ*mcs1* were highly susceptible to oxidative stress.

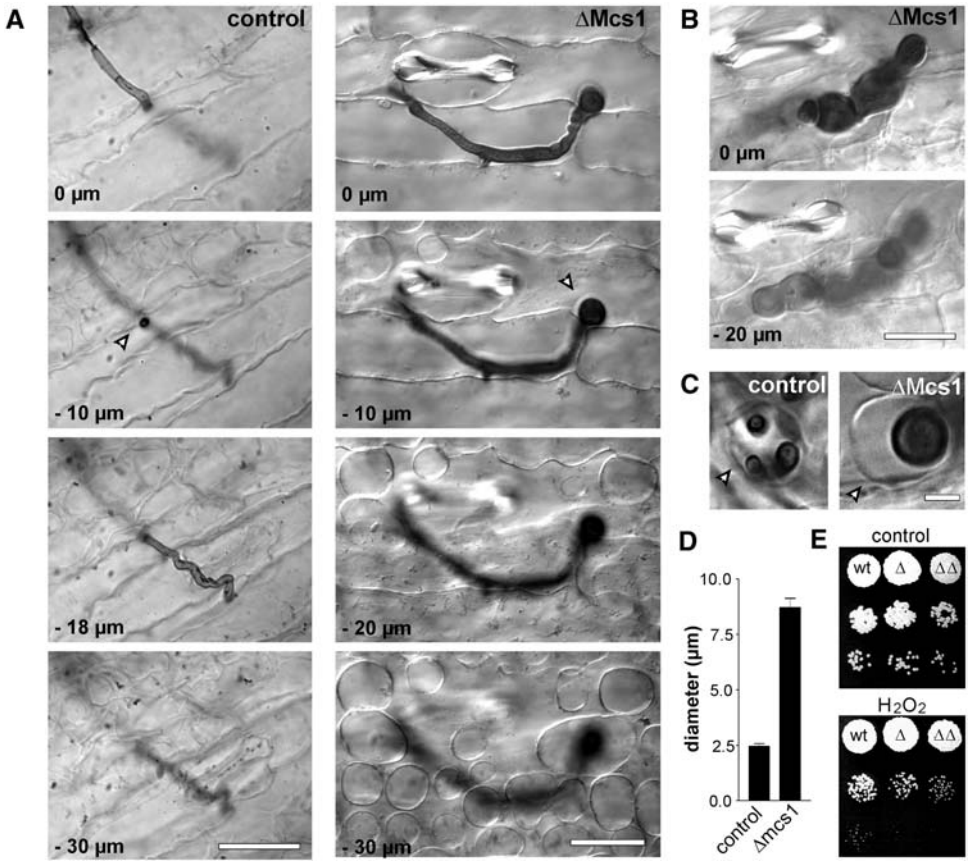

Figure 9. Defects of Δ*mcs1* Hyphae in Early Plant Infection.

(A) Series of *Z* axis projections showing the initial infection state of the wild type (control) and Δ*mcs1* mutants. One day after infection, wild-type hyphae enter the plant epidermis without obvious morphological differentiation (arrowhead, −10 μm). By contrast, even at 3 d after infection, most Δ*mcs1* hyphae fail to invade the host tissue or they reach just into the upper layer (arrowhead, −10 μm). Note that Δ*mcs1* mutants are heavily swollen at the infection site. Distance in the *Z*-direction is given in micrometers. Bars = 20 μm.

(B) Those hyphae that entered the plant tissue did not continue directed growth but formed large aggregates of rounded and swollen cells. Distance in the *Z*-direction is given in micrometers. Bar = 20 μm.

(C) Invading mutant hyphae are able to grow inside plant cells (the plant cell wall is indicated by arrowheads) but are thicker than control cells. This indicates that Mcs1 is not needed for invasion but becomes essential for hyphal morphogenesis and directed growth. Bar = 5 μm.

(D) Quantitative analysis of the diameter of control and Δ*mcs1* hyphae in planta. In the absence of Mcs1, the hyphal diameter is increased significantly, indicating that cells are able to grow but have lost their polarity. Values are given as means ± SE (n = 10 to 11 appressoria).

(E) On agar plates, the growth of wild-type FB2 cells, Δ*mcs1*, and Δ*mcs1* Δ*chs6* mutants was not different. In the presence of ~0.0035% (v/v) H_2O_2 oxidative stress, the growth of control cells and mutants was impaired, but again no strong difference between control and mutant strains was detected.

However, at inhibitory sublethal concentrations (~0.03%, v/v), mutants and control strains showed similar growth inhibition (Figure 9E). This indicated that the absence of virulence of Δ*mcs1* mutants is not the result of a plant defense reaction. In summary, these data suggest that Mcs1 is required for directed hyphal growth inside plants, a result that is most surprising considering that Δ*mcs1* mutants did not show any polarity or growth defects in yeast-like cells, mating tubes, and dikaryotic hyphae ex planta.

DISCUSSION

U. maydis Contains Eight CHSs

Previous work on CHS in *U. maydis* led to the description and partial characterization of six CHSs (Gold and Kronstad, 1994; Xoconostle-Cazares et al., 1996, 1997; Garcerá-Teruel et al., 2004) that covered all five classes of these enzymes. In this study, we made use of the recently published genome of *U. maydis* and identified two additional CHSs, which raises the number of CHS genes to eight. Such high numbers appear to be typical for filamentous fungi (Miyazaki and Ootaki, 1997; Choquer et al., 2004), whereas the yeasts *Schizosaccharomyces pombe* and *S. cerevisiae* have only two and three CHSs, respectively (Cabib et al., 2001; Matsuo et al., 2004). It was argued that the high number of CHSs in filamentous and dimorphic fungi reflects their more complex life cycles and developmental programs, by which they colonize very different ecological niches ranging from soil to host tissue. However, *Candida albicans* grows in three different morphologies (Sudbery et al., 2004) but contains only four CHSs (Munro et al., 2003). Therefore, the number of CHSs does not necessarily reflect morphological complexity. Indeed, our data show that all eight CHSs of *U. maydis* are expressed in yeast-like cells and in hyphae. Most CHSs localized to the septa of yeast-like cells and hyphae, whereas at least four CHSs were concentrated at the growth region. This clearly suggests that CHSs cooperate in yeast-like cells, hyphae, and most likely during plant infection, but the importance of individual CHSs varies depending on the developmental stage. Such a concept is supported by the fact that deletion of single CHS genes often has no obvious phenotypes, whereas double or triple mutants have major phenotypes (Wang et al., 2001), and the increased morphological defects of the double mutant in class V CHSs (ΔMcs1 ΔChs6) argue similarly. On the other hand, double mutants in *U. maydis chs3* and *chs4* were without prominent phenotypes (Chavez-Ontiveros et al., 2000). However, our localization data indicate that at least six CHSs participate in septation in yeast-like cells and hyphae and at least four CHSs cooperate to support polar growth. This strongly suggests that multiple CHSs share similar functions and substitute for each other. Such cooperation could explain why mutants in *chs4* and *chs1*, for which transcription is induced by >11-fold in hyphae, are without any phenotype in hyphae, although Δ*chs4* mutants are attenuated in virulence. Further genetic analysis of mutants deleted in both *chs1* and *chs4* and even more CHS mutants will be needed to gain deeper insight into the functional relationship of CHSs in *U. maydis*.

The Polar Class VI CHSs Chs5 and Chs7 Are Essential for the Morphology of Yeast-Like Cells, Mating Tubes, and Dikaryotic Hyphae

Fungal morphology depends on the integrity of the rigid cell wall that resists internal osmotic pressure (Harold, 2002). Chitin confers stability to the cell wall; therefore, it is not surprising that CHS mutants are often defective in cell morphology (Shaw et al., 1991; Borgia et al., 1996; Munro et al., 2001; Muller et al., 2002). We describe here that Chs5 and Chs7 are most important for the morphology of yeast-like cells, conjugation hyphae, and dikaryotic hyphae of *U. maydis* (Figure 10). Moreover, both Chs5

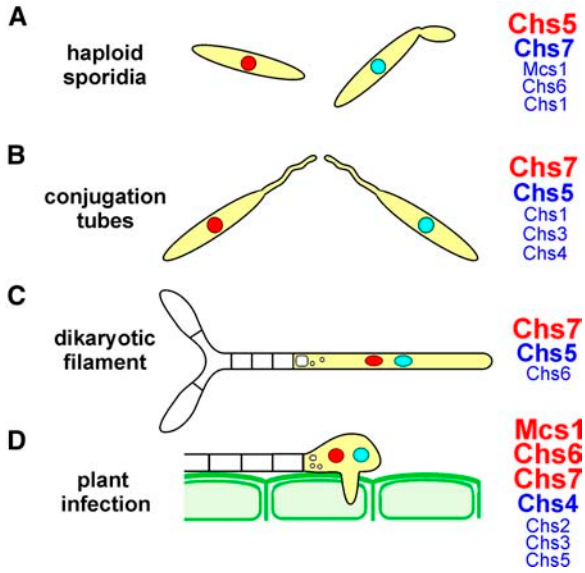

Figure 10. Overview of the Importance of CHSs in Different Life Cycle Stages of *U. maydis*.

The cellular importance of each CHS is reflected by the size of its name. **(A)** Haploid yeast-like cells grow by polar budding, and Chs5 is essential for their morphology. Δ*chs7* cells show an additional cell separation defect, and Δ*mcs1* mutants are often thicker and show polar swellings, indicating that these CHSs also participate in morphogenesis. Finally, Δ*chs1*, Δ*chs5*, Δ*chs6*, Δ*chs7*, and Δ*mcs1* are hypersensitive against Nikkomycin Z, which apparently inhibits CHS activity at the growing tip. This finding suggests that these CHSs support the tip growth of yeast-like cells.
(B) Pathogenic development is initiated by the formation of conjugation hyphae. Chs5 and Chs7 are essential for the formation of these tubes, whereas Chs1, Chs3, and Chs4 are of minor importance. However, only Chs7 activity is required for the proper morphology of mating tubes.
(C) Chs7 is essential for the proper morphology and growth of dikaryotic hyphae, whereas ΔChs5 shows a significant delay in the growth of dikaryotic hyphae. Again, Chs6 participates in hyphal growth, but its activity is of minor importance.
(D) Only Chs6, Chs7, and Mcs1 are essential during the infection process, whereas Chs2, Chs3, Chs4, and Chs5 play only minor roles that become crucial when the plant grows under optimal conditions. In part, the pathogenicity of Δ*chs7* mutants could be restored when solopathogenic strains were used, indicating that the reduced virulence is partially attributable to the described mating defects. By contrast, Mcs1 activity becomes crucial when the fungus enters the plant.

and Chs7 show reduced virulence, although null mutants were still able to induce small tumors. Both genes belong to class IV CHSs, suggesting that members of this class are essential for fungal morphogenesis. Indeed, it was shown that class IV CHSs also have important roles in *S. cerevisiae* (Shaw et al., 1991) and *C. albicans* (Mio et al., 1996), which emphasizes the importance of this class of CHS in fungi. However, in *Neurospora crassa*, deletion of class IV CHSs was without significant effect (Din et al., 1996). This raises doubts about specific cellular functions of individual classes of CHS. Indeed, it was reported that class III CHSs are not important in *U. maydis* (Gold and Kronstad, 1994) and apparently do not even exist in *Phycomyces blakesleeanus* (Miyazaki and Ootaki, 1997), whereas this class has crucial functions in morphogenesis in *Aspergillus oryzae* (Muller et al., 2002) and *Aspergillus nidulans* (Borgia et al., 1996). The situation is even more complicated by the fact that CHSs of different classes cooperate to mediate conidiation and hyphal growth (Motoyama et al., 1996; Fujiwara et al., 2000) or fungal virulence (Wang et al., 2001). Therefore it appears impossible to assign common cellular importance to CHSs that belong to the same class. However, our data demonstrate that *U. maydis* contains four CHSs, two of class IV and two of class V, that perform important roles in morphogenesis and pathogenicity, whereas class I, II, and III are of minor importance (Figure 10).

The Class V CHS Mcs1 Is Essential for Penetration of the Host Epidermis

Members of class V CHSs usually contain a large N-terminal domain that has significant homology with myosin motor domains, and only Chs6 in *U. maydis* lacks this region (Xoconostle-Cazares et al., 1997). Here, we report the existence of *mcs1*, a second class V gene in *U. maydis* that encodes a complete myosin-CHS. Interestingly, myosin-CHSs are found in filamentous fungi (Aufauvre-Brown et al., 1997; Fujiwara et al., 1997), including the plant pathogens *F. oxysporum* (Madrid et al., 2003) and *Botrytis cinerea* (Choquer et al., 2004), as well as human pathogens, such as *Paracoccidioides brasiliensis* (Nino-Vega et al., 2004) and *Wangiella dermatitidis* (Liu et al., 2004), but they are absent from the yeast *S. cerevisiae* and *S. pombe*. This suggests that myosin-CHSs may be of particular importance for fungal hyphae (Roncero, 2002). However, Mcs1 participates in morphogenesis of the yeast-like stage, as Δ*mcs1* Δ*chs6* double mutants have a significant defect in cell morphology. This suggests that both class V CHSs have overlapping functions in *U. maydis*. Neither Chs6 nor Mcs1 was important for the hyphal stage of *U. maydis*, namely, the conjugation and dikaryotic hyphae (Figure 10). This is surprising, because deletion in class V CHSs in other fungi led to swelling of the hypha (Horiuchi et al., 1999; Madrid et al., 2003) or the hyphal tip (Amnuaykanjanasin and Epstein, 2003) and irregular septation (Horiuchi et al., 1999). One could argue that the lack of a morphology phenotype in Δ*mcs1* hyphae was attributable to a cell cycle–specific inactivation in the *b*-dependent hyphae, which are arrested in G2 phase. However, cAMP-dependent Δ*adr1* hyphae that grow filamentously but are not arrested in the cell cycle (Dürrenberger et al., 1998) also show no obvious mutant phenotype. Interestingly, quantitative staining of chitin in control strain SG200 and SG200ΔMcs1 revealed that mutant hyphae lack an apical chitin cap, suggesting that Mcs1 indeed participates in wall synthesis in hyphae. However, this activity is not essential for hyphal morphology, suggesting that other CHSs compensate for the loss of Mcs1 in hyphae. This notion is supported by a recent report on a triple CHS-deletion mutant in *A. nidulans* that suggests that the myosin-CHS *csmA* has a functional overlap with a class I and a class II CHS (Yamada et al., 2005). In summary, our results demonstrate that myosin-CHS is not essential for hyphal morphology in *U. maydis*, in contrast with reports on other fungi. Notably, these fungi belong to the ascomycetes, whereas *U. maydis* is a basidiomycete. This raises the possibility that the role of Mcs1 in hyphal growth is taxon-specific. Further studies on other basidiomycete fungi will be required to gain support for this notion.

Interestingly, Mcs1 is crucial for the initial steps of plant infection. Ex planta, Δ*mcs1* hyphae grew straight (Figure 6). Consistently, straight hyphae were found on the plant surface (Figure 9A, ΔMcs1, 0 μm), whereas mutant hyphae swell markedly after entering the epidermis and form large globular aggregates that are unable to invade deeper layers of the host tissue. A similar role of class V CHSs in plant pathogenicity was recently described in *F. oxysporum* (Madrid et al., 2003). Null mutants in ChsV are able to invade tomato plants, but the infection does not proceed, apparently because of a hypersensitivity of the mutant hyphae against early plant defense reactions, including oxidative stress and chemical attack by a phytoanticipin (Madrid et al., 2003). However, neither Δ*mcs1* nor Δ*mcs1* Δ*chs6* yeast-like cells exhibit a higher sensitivity to H_2O_2-induced oxidative stress. Thus, we do not find support for the idea that Mcs1 activity protects the fungal cell from plant defense. Alternatively, we consider it possible that dikaryotic hyphae modify their cell walls after invading the plant epidermis and that Mcs1 activity could become essential at this stage. In other words, Δ*mcs1* invading hyphae might have a weaker cell wall, which could result in the observed swellings and the inability to further invade the host. This notion is supported by a recent study on another class V CHS in the human pathogen *W. dermatitidis* (Liu et al., 2004). Δ*WdCHS5* strains show reduced virulence, but this was restored by decreased osmotic stress, suggesting that defects in the integrity of the cell wall are responsible for the decreased pathogenicity of these mutants. The crucial role of Mcs1 in the morphology of hyphae in planta implies that *U. maydis* undergoes major cell wall rearrangements upon contact with the host plant. Interestingly, it was recently reported that in several plant pathogenic fungi, the cell wall is modified upon entry into the host tissue, and it was speculated that the de-*N*-acetylation of chitin is part of a defense strategy that protects the fungal cell from plant attack (Deising and Siegrist, 1995; Gueddari et al., 2002). Therefore, we consider it possible that de novo synthesis of chitin by Mcs1 participates in wall modification in early infection steps of *U. maydis*. It will be a fascinating future challenge to further our understanding of the morphological transition during plant invasion.

Polar Localization Correlates with Cellular Importance

Fungi typically grow at the hyphal tip, where cell expansion and cell wall synthesis occur (Gow, 1995). Therefore, it is expected

that CHSs are concentrated at the growing apex, but direct evidence for such localization in fungal hyphal tips is rare (Archer, 1977; Sietsma et al., 1996). We fused GFP to the endogenous copy of all CHSs and show here that the fusion proteins of the class IV enzymes Chs5 and Chs7, as well as the class V members Chs6 and Mcs1, are concentrated at the growing tip of yeast-like cells and hyphae, whereas Chs3 and Chs4, as well as Chs5-, Chs6-, Chs7-, and Mcs1-GFP/YFP fusion proteins localized to septa, where new cell wall is synthesized. Indeed, the GFP fusion proteins either rescued the deletion phenotype (Mcs1-GFP) or did not induce any morphological defect (Chs5-GFP, Chs6-GFP, and Chs7-GFP), suggesting that they are biologically functional. Thus, it is likely that their localization indicates the region of their activity. However, it is important to note that the polar CHSs have additional roles in other parts of the cell, as deletion of *chs5*, *chs6*, and *mcs1* led to morphological alterations in the mother cell, whereas Δ*chs7* mutants showed aberrant chitin distribution in the mother cell and cell separation defects. This suggests that these CHSs participate in wall synthesis in the mother cell. Nevertheless, the strong concentration of CHSs at the growing tip indicates that their major function is to support polar fungal growth. Interestingly, our data also demonstrate that the polar localization correlates with high cellular importance. Class IV and class V CHSs were found at the growing tips, and these CHSs are most important for the morphology of yeast cells and hyphae as well as later stages during plant infection (Figure 10).

Conclusions

The genome of *U. maydis* encodes eight CHSs that are expressed during yeast-like and hyphal growth. Six CHSs are located at the septa, whereas four CHSs that belong to class IV and V are concentrated at the tip. Interestingly, the class IV CHSs are important for the morphology of yeast and hyphal cells, whereas the two class V CHSs are crucial for pathogenicity (Figure 10). The unsuccessful plant infection of Δ*mcs1* mutants is apparently attributable to a severe swelling of the hypha during early infection. This loss of directed hyphal growth is surprising, because Δ*mcs1* dikaryotic hyphae were without obvious defects. However, our results demonstrate that yeast-like cells require Chs5 for proper morphology, whereas hyphal stages were not affected by deletion of *chs5*. These results suggest that tip growth of yeast-like cells, dikaryotic hyphae, and hyphal growth inside the plant are supported by different CHSs. Thus, we conclude that hyphal growth inside and outside of the plant is not the same, indicating that the developmental stages of *U. maydis* are characterized by unrecognized molecular and structural differences.

METHODS

Strains, Plasmids, and Growth Conditions

Strains FB1 (*a1b1*), FB2 (*a2b2*), FB6a (*a2b1*), FB6b (*a1b2*), and SG200 (*a1 mfa2 bW2 bE1*) have been described (Banuett and Herskowitz, 1989; Bölker et al., 1995) (details of strain genotypes are listed in Table 1). Strain SG1 (Δ*chs1*) and the plasmid pUC18-chs2 were obtained from J. Kronstad, and mating-compatible strains FB1ΔChs6 and AG2 (Δ*chs6*) were kindly provided by J. Ruiz-Herrera. Deletion of *chs3*, *chs4*, *chs5*, *chs6*, *chs7*, and *mcs1* was done by homologous replacement of the corresponding gene with either a bleomycin or a hygromycin resistance cassette in strains FB1, FB2, SG200, FB1ΔChs6, and AG2 according to described protocols (Brachmann et al., 2004; Kämper, 2004). This resulted in strains FB2ΔChs3, FB2ΔChs4, FB2ΔChs5, FB1ΔChs7, FB2ΔChs7, FB1ΔMcs1, FB2ΔMcs1, FB1ΔChs6ΔMcs1, IW 46 (Δ*chs6* Δ*mcs1*), SG200ΔChs5, SG200ΔChs6, SG200ΔChs7, and SG200ΔMcs1. The compatible deletion strains of *chs1* (IW 248 and IW 249), *chs2* (IW 253 and IW 254), *chs3* (IW 101 and IW 102), *chs4* (IW 84 and IW 85), and *chs5* (IW 89) were generated by segregation analysis of teliospores after plant infection with FB1 (*a1b1*) and the corresponding deletion strain. The mating type was determined by monitoring filamentous growth in crossings with the wild-type strains FB1 (*a1b1*), FB2 (*a2b2*), FB6a (*a2b1*), and FB6b (*a1b2*). For the in vivo localization of CHS, the 3′ end of the gene was determined by nested PCR on a λgt10 cDNA library that contained oligo(dTT)-primed 3′ end sequences (Schauwecker et al., 1995). Plasmids pChs1GFP, pChs2GFP, pChs3GFP, pChs4GFP, pChs5GFP, pChs6GFP, pChs7YFP, and pMcs1YFP were constructed by fusing 500 to 800 bp of the 3′ end of the corresponding gene to the N terminus of *gfp* or *yfp* flanked by a bleomycin resistance cassette. This was followed by 500 to 800 bp of the 3′ untranslated region of the genes. Flanking regions were generated by PCR from genomic DNA. Successful cloning was confirmed by sequencing. These plasmids were integrated into the endogenous loci of FB2 by homologous recombination, resulting in strains FB2Chs3GFP, FB2Chs4GFP, FB2Chs5GFP, FB2Chs6GFP, FB2Chs7YFP, and FB2Mcs1YFP. pChs7YFP and pMcs1YFP have also been integrated into strain AB33, which grows filamentously in nitrate-containing medium (Brachmann et al., 2001), resulting in strains AB33Chs7YFP and AB33Mcs1YFP. Successful homologous recombination was confirmed by DNA gel blotting. Strain SG200ΔMcs1OGMcs1 was generated by ectopic integration of the plasmid pOGMcs1, containing *mcs1-gfp* under the control of the constitutive *otef* promoter. The Δ*adr1* strains (Table 1) were generated by replacing *adr1* with the nourseothricin resistance cassette. To rescue the deletion phenotype of Δ*chs5* strains, the plasmid pChs5 was cloned, harboring the backbone of the autonomous replication plasmid pNEBUH with the *chs5* gene under the control of the native promoter, resulting in strain FB2ΔChs5pChs5. Control cells contained the empty vector pNEBUH. To rescue the morphology defects of Δ*chs7* cells and the defects in filamentous growth of compatible Δ*chs7* strains, the plasmid pChs7 was cloned harboring the backbone of the autonomous replication plasmid pNEBUC with the *chs7* gene under the control of the native promoter, resulting in strains FB1ΔChs7pChs7 and FB2Chs7pChs7. Control cells contained the empty vector pNEBUC. Strains were grown at 28°C in CM-G (Holliday, 1974). Solid medium contained 2% (w/v) bacto-agar. Strains were crossed on potato dextrose plates containing 1% charcoal (Holliday, 1974) and observed after 1 and 2 d. To localize Chs1GFP, Chs2GFP, Chs3GFP, Chs4GFP, Chs5GFP, and Chs6GFP in dikaryotic hyphae, the compatible strains FB2Chs1GFP, FB2Chs2GFP, FB2Chs3GFP, FB2Chs4GFP, FB2Chs5GFP, and FB2Chs6GFP were mixed with FB1 and incubated on charcoal plates for 1 to 2 d. Filamentous growth of AB33Chs7YFP and AB33Mcs1YFP was induced by shifting cells grown in CM-G to nitrate minimal medium/1% glucose (Holliday, 1974), followed by 8 to 12 h of growth at 28°C. To determine the growth rate, CHS deletion strains were grown overnight in CM-G and subsequently adjusted to $OD_{600} = 0.5$. Fourteen milliliters of fresh medium was inoculated with 1 mL of cell suspension, and cells were cultivated for an additional 2 h at 28°C, followed by OD_{600} measurements every hour. Doubling times were calculated after nonlinear regression using the program Prism (GraphPad).

DNA and RNA Procedures and Real-Time PCR

Standard molecular techniques were used. Transformation of *U. maydis* was done as described (Schulz et al., 1990). Isolation of *U. maydis* DNA was done according to published protocols (Hoffman and Winston, 1987).

RNA was isolated from the filamentously growing strain AB33 that expresses a compatible bE/bW heterodimer (a transcription factor that regulates hyphal growth) and therefore forms a dikaryotic filament (Brachmann et al., 2001). The expression data of AB33 were compared with those of the control strain AB34 that produces noncompatible b factors and therefore does not form hyphae (Brachmann et al., 2001). RNA was prepared from liquid cultures using Trizol reagents (Invitrogen) according to the manufacturer's instructions. RNA gel blots were probed using radioactively labeled PCR products amplified with open reading frame–specific primers from genomic DNA. Radioactive labeling was performed with the NEBlot kit (New England Biolabs). Membranes were stained for 5 min in 200 mg/mL methylene blue in 300 mM sodium acetate and subsequently washed with water to assess equal loading and transfer. A PhosphorImager (Storm 840; Molecular Dynamics) and the program ImageQuant (Molecular Dynamics) were used for visualization and quantification of radioactive signals. Real-time PCR was performed on a Roche LightCycler system (Roche). Relative gene expression levels were determined using a one-step QuantiTect SYBR Green RT-PCR assay (Qiagen) according to the manufacturer's protocol. One hundred nanograms of the RNA samples was used as a template for the reaction. Before RT-PCR assays, quantitative and qualitative analyses of the RNA samples were performed using a Bioanalyzer with an RNA 6000 Nano LabChip kit (Agilent). Cycling reactions were performed three times, and negative controls (in the absence of template) were included. First-strand synthesis was performed at 50°C for 20 min, followed by denaturation at 95°C for 10 min, 40 cycles for 20 s at 59 to 65°C, and extension at 70°C for 40 s. After each PCR, the specificity of the amplifications was verified and the threshold cycle above background was calculated using the Roche LightCycler software. To verify the specificity of the RT-PCR, the size of the amplicons was analyzed by high-resolution sizing of DNA fragments using a Bioanalyzer 2100 system and a LabChip DNA 100 assay (Agilent).

Phylogenetic Analysis

Alignments were made with ClustalX (Thompson et al., 1997). Phylogenetic dendrograms were constructed using MEGA 2.1 (www.megasoftware.net) (Kumar et al., 2001), with the minimum evolution algorithms using 1000 bootstrap replications. The actual alignment is given in Supplemental Table 1 online. Analysis of transmembrane domains was done using Sosui (www.expasy.ch). The sequences of all CHSs were obtained from the genome sequence of *U. maydis* initially provided by Bayer CropScience and recently published by the Broad Institute (www.broad.mit.edu/annotation/fungi/ustilago_maydis/index.html). Sequences of myosin-CHS of *Phanerochaete crysogenum* were obtained from the Department of Energy Joint Genome Institute (www.jgi.doe.gov), and those of *Neurospora crassa* were from the Whitehead Institute (www.broad.mit.edu/annotation/fungi/neurospora).

Drug Treatment and Pheromone Stimulation Experiment

Nikkomycin Z (Sigma-Aldrich) was added to growing cultures at a final concentration of 5 μM. After 1 to 2 h at 28°C, cells were microscopically analyzed. Inhibitory effects on growth at 28°C for 2 d were analyzed on CM-G plates supplemented with 0.1 to 5 μM Nikkomycin Z. For pheromone response studies, synthetic pheromone (Szabo et al., 2002) was added to 500 μL of cell suspension (OD_{600} between 0.4 and 1) in a 2-mL reaction tube and incubated at 20°C and 200 rpm for 8 or 14 h, followed by microscopic analysis.

Microscopy, Live Cell Observation, and Staining Procedures

Light microscopy was done using a Zeiss Axioplan II microscope (Zeiss). For epifluorescence, standard fluorescein isothiocyanate, 4′,6-diamidino-2-phenylindole, and rhodamine filter sets were used. Digital images or sequences were captured with a cooled charge-coupled device camera (CoolSNAP HQ; Roper Scientific). *Z* axis imaging stacks were generated by acquiring images with 100-nm step intervals using a CoolSNAP-HQ charge-coupled device camera (Photometrics) and the motorized stage of the Axioplan II microscope, both controlled by the imaging software MetaMorph (Universal Imaging). For observation of cells from liquid culture, logarithmically growing cells were embedded in 1% low-melt agarose and mounted on slides. Microscopic preparations were observed no longer than 10 min to prevent defects attributable to oxygen depletion. Rhodamine-conjugated wheat germ agglutinin and Calcofluor staining was done as described previously (Wedlich-Söldner et al., 2000). All measurements and image processing, including adjustment of brightness, contrast and γ values, and two-dimensional deconvolution, were performed with MetaMorph (Universal Imaging) and Photoshop (Adobe). Statistical analysis by two-tailed *t* test at α: 0.05 was performed using Prism (GraphPad). All values are given as means ± SD unless stated otherwise.

Plant Pathogenicity Assays and Observation of Fixed Fungal Hyphae in Plant Tissue

Plant infection was performed as described (Gillissen et al., 1992). The percentage of the maize (*Zea mays*) plants having one or more tumors that were recognized by touching was counted at 12 to 14 d after infection in an initial experiment regardless of tumor size. In a second set of experiments, a newly built greenhouse was used and plants were infected as before. Tumor development was monitored on a daily basis, and the fresh weight of tumors was determined after 14 d. Chlorazole black E staining was done as described previously (Brachmann et al., 2003). In brief, infected plant material was harvested 1 and 3 d after infection, incubated in ethanol and KOH to clear the material, and subsequently stained with chlorazole black.

Accession Numbers

Sequence data from this article can be found in the GenBank/EMBL data libraries under accession numbers M82958 for *chs1*, M82959 for *chs2*, X87748 for *chs3*, X87749 for *chs4*, AF030553 for *chs5*, AF030554 for *chs6*, XP_761627 for *chs7*, and XP_754288 for *mcs1*.

Supplemental Data

The following material is available in the online version of this article.

Supplemental Table 1. Sequence Alignment of CHSs.

ACKNOWLEDGMENTS

We are very grateful to Petra Happel, Uta Fuchs, Isabel Manns, and Jan Heiko Lenz for technical help. Regine Kahmann is acknowledged for helpful comments on the manuscript. We also thank Jim Kronstad, Jose Ruiz-Herrera, and Michael Feldbrügge for providing strains and plasmids. Finally, we thank the anonymous referees for excellent suggestions.

Received August 25, 2005; revised October 5, 2005; accepted October 20, 2005; published November 28, 2005.

REFERENCES

Amnuaykanjanasin, A., and Epstein, L. (2003). A class V chitin synthase gene, chsA is essential for conidial and hyphal wall strength in the fungus *Colletotrichum graminicola* (*Glomerella graminicola*). Fungal Genet. Biol. **38,** 272–285.

Archer, D.B. (1977). Chitin biosynthesis in protoplasts and subcellular fractions of *Aspergillus fumigatus.* Biochem. J. **164,** 653–658.

Aufauvre-Brown, A., Mellado, E., Gow, N.A.R., and Holden, D.W. (1997). *Aspergillus fumigatus chsE*: A gene related to CHS3 of *Saccharomyces cerevisiae* and important for hyphal growth and conidiophore development but not pathogenicity. Fungal Genet. Biol. **21,** 141–152.

Banuett, F., and Herskowitz, I. (1989). Different a alleles of *Ustilago maydis* are necessary for maintenance of filamentous growth but not for meiosis. Proc. Natl. Acad. Sci. USA **86,** 5878–5882.

Banuett, F., and Herskowitz, I. (1996). Discrete developmental stages during teliospore formation in the corn smut fungus, *Ustilago maydis.* Development **122,** 2965–2976.

Bölker, M., Genin, S., Lehmler, C., and Kahmann, R. (1995). Genetic regulation of mating and dimorphism in *Ustilago maydis.* Can. J. Bot. **73,** 320–325.

Borgia, P.T., Iartchouk, N., Riggle, P.J., Winter, K.R., Koltin, Y., and Bulawa, C.E. (1996). The chsB gene of *Aspergillus nidulans* is necessary for normal hyphal growth and development. Fungal Genet. Biol. **20,** 193–203.

Brachmann, A., Konig, J., Julius, C., and Feldbrugge, M. (2004). A reverse genetic approach for generating gene replacement mutants in *Ustilago maydis.* Mol. Genet. Genomics **272,** 216–226.

Brachmann, A., Schirawski, J., Muller, P., and Kahmann, R. (2003). An unusual MAP kinase is required for efficient penetration of the plant surface by *Ustilago maydis.* EMBO J. **22,** 2199–2210.

Brachmann, A., Weinzierl, G., Kämper, J., and Kahmann, R. (2001). Identification of genes in the bW/bE regulatory cascade in *Ustilago maydis.* Mol. Microbiol. **42,** 1047–1063.

Bracker, C.E., Ruiz-Herrera, J., and Bartnicki-Garcia, S. (1976). Structure and transformation of chitin synthetase particles (chitosomes) during microfibril synthesis in vitro. Proc. Natl. Acad. Sci. USA **73,** 4570–4574.

Brundett, M., Bougher, N., Dell, B., Grove, T., and Malajcuk, N. (1996). Working with Mycorrhizas in Forestry and Agriculture. (Canberra, Australia: Australian Centre for International Agricultural Research), Monograph 32.

Cabib, E., Roh, D.-H., Schmidt, M., Crotti, L.B., and Varma, A. (2001). The yeast cell wall and septum as paradigms of cell growth and morphogenesis. J. Biol. Chem. **276,** 19679–19682.

Chavez-Ontiveros, J., Martinez-Espinoza, A.D., and Ruiz-Herrera, J. (2000). Double chitin synthetase mutants from the corn smut fungus *Ustilago maydis.* New Phytol. **146,** 335–341.

Choquer, M., Boccara, M., Goncalves, I.R., Soulie, M.C., and Vidal-Cros, A. (2004). Survey of the *Botrytis cinerea* chitin synthase multigenic family through the analysis of six euascomycetes genomes. Eur. J. Biochem. **271,** 2153–2164.

Deising, H.B., and Siegrist, J. (1995). Chitin deacetylase activity of the rust *Uromyces viciae-fabae* is controlled by fungal morphogenesis. FEMS Microbiol. Lett. **127,** 207–212.

Din, A.B., Specht, C.A., Robbins, P.W., and Yarden, O. (1996). Chs-4, a class IV chitin synthase gene from *Neurospora crassa.* Mol. Gen. Genet. **250,** 214–222.

Duran, A., Cabib, E., and Bowers, B. (1979). Chitin synthetase distribution on the yeast plasma membrane. Science **203,** 363–365.

Dürrenberger, F., Wong, K., and Kronstad, J.W. (1998). Identification of a cAMP-dependent protein kinase catalytic subunit required for virulence and morphogenesis in *Ustilago maydis.* Proc. Natl. Acad. Sci. USA **95,** 5684–5689.

Feldbrügge, M., Kämper, J., Steinberg, G., and Kahmann, R. (2004). Regulation of mating and pathogenic development in *Ustilago maydis.* Curr. Opin. Microbiol. **7,** 666–672.

Fujiwara, M., Horiuchi, H., Ohta, A., and Takagi, M. (1997). A novel fungal gene encoding chitin synthase with a myosin motor-like domain. Biochem. Biophys. Res. Commun. **236,** 75–78.

Fujiwara, M., Ichinomiya, M., Motoyama, T., Horiuchi, H., Ohta, A., and Takagi, M. (2000). Evidence that the *Aspergillus nidulans* class I and class II chitin synthase genes, *chsC* and *chsA*, share critical roles in hyphal wall integrity and conidiophore development. J. Biochem. (Tokyo) **127,** 359–366.

Garcerá-Teruel, A., Xoconostle-Cazares, B., Rosas-Quijano, R., León-Ramírez, C., Specht, C.A., Sentandreu, R., and Ruiz-Herrera, J. (2004). Loss of virulence in *Ustilago maydis* mutants affected in the chitin synthase gene *umchs6.* Res. Microbiol. **155,** 87–97.

Garcia-Muse, T., Steinberg, G., and Perez-Martin, J. (2003). Pheromone-induced G2 arrest in the phytopathogenic fungus *Ustilago maydis.* Eukaryot. Cell **2,** 494–500.

Gaughran, J.P., Lai, M.H., Kirsch, D.R., and Silverman, S.J. (1994). Nikkomycin Z is a specific inhibitor of *Saccharomyces cerevisiae* chitin synthase isozyme Chs3 in vitro and in vivo. J. Bacteriol. **176,** 5857–5860.

Gillissen, B., Bergemann, J., Sandmann, C., Schröer, B., Bölker, M., and Kahmann, R. (1992). A two-component regulatory system for self/non-self recognition in *Ustilago maydis.* Cell **68,** 647–657.

Gold, S., and Kronstad, J. (1994). Disruption of two genes for chitin synthase in the phytopathogenic fungus *Ustilago maydis.* Mol. Microbiol. **11,** 897–902.

Gow, N.A.R. (1995). Tip growth and polarity. In The Growing Fungus, N.A.R. Gow and G.M. Gadd, eds (London: Chapman & Hall), pp. 277–299.

Gueddari, N.E.E., Rauchhaus, U., Moerschbacher, B.M., and Deising, H.B. (2002). Developmentally regulated conversion of surface-exposed chitin to chitosan in cell walls of plant pathogenic fungi. New Phytol. **156,** 103–112.

Harold, F.M. (2002). Force and compliance: Rethinking morphogenesis in walled cells. Fungal Genet. Biol. **37,** 271–282.

Hoffman, C.S., and Winston, F. (1987). A ten-minute DNA preparation from yeast efficiently releases autonomous plasmids for transformation of *Escherichia coli.* Gene **57,** 267–272.

Holliday, R. (1974). *Ustilago maydis.* In Handbook of Genetics, R.C. King, ed (New York: Plenum Press), pp. 575–595.

Horiuchi, H., Fujiwara, M., Yamashita, S., Ohta, A., and Takagi, M. (1999). Proliferation of intrahyphal hyphae caused by disruption of *csmA*, which encodes a class V chitin synthase with a myosin motor-like domain in *Aspergillus nidulans.* J. Bacteriol. **181,** 3721–3729.

Ichinomiya, M., Horiuchi, H., and Ohta, A. (2002). Different functions of the class I and class II chitin synthase genes, chsC and chsA, are revealed by repression of chsB expression in *Aspergillus nidulans.* Curr. Genet. **42,** 51–58.

Kämper, J. (2004). A PCR-based system for highly efficient generation of gene replacement mutants in *Ustilago maydis.* Mol. Genet. Genomics **271,** 103–110.

Kumar, S., Tamura, K., Jakobsen, I.B., and Nei, M. (2001). MEGA2: Molecular evolutionary genetics analysis software. Bioinformatics **17,** 1244–1245.

Leal-Morales, C.A., Bracker, C.E., and Bartnicki-Garcia, S. (1988). Localization of chitin synthetase in cell-free homogenates of *Saccharomyces cerevisiae*: Chitosomes and plasma membrane. Proc. Natl. Acad. Sci. USA **85,** 8516–8520.

Leal-Morales, C.A., Bracker, C.E., and Bartnicki-Garcia, S. (1994). Subcellular localization, abundance and stability of chitin synthetases 1 and 2 from *Saccharomyces cerevisiae.* Microbiology **140,** 2207–2216.

Lee, J.I., Choi, J.H., Park, B.C., Park, Y.H., Lee, M.Y., Park, H.M., and Maeng, P.J. (2004). Differential expression of the chitin synthase

genes of *Aspergillus nidulans*, chsA, chsB, and chsC, in response to developmental status and environmental factors. Fungal Genet. Biol. **41,** 635–646.

Liu, H., Kauffman, S., Becker, J.M., and Szaniszlo, P.J. (2004). *Wangiella* (*Exophiala*) *dermatitidis* WdChs5p, a class V chitin synthase, is essential for sustained cell growth at temperature of infection. Eukaryot. Cell **3,** 40–51.

Madrid, M.P., Di Pietro, A., and Roncero, M.I. (2003). Class V chitin synthase determines pathogenesis in the vascular wilt fungus *Fusarium oxysporum* and mediates resistance to plant defence compounds. Mol. Microbiol. **47,** 257–266.

Martinez, J.P., and Gozalbo, D. (1994). Chitin synthetases in *Candida albicans*: A review on their subcellular distribution and biological function. Microbiologia **10,** 239–248.

Matsuo, Y., Tanaka, K., Nakagawa, T., Matsuda, H., and Kawamukai, M. (2004). Genetic analysis of *chs1*$^+$ and *chs2*$^+$ encoding chitin synthases from *Schizosaccharomyces pombe.* Biosci. Biotechnol. Biochem. **68,** 1489–1499.

Mio, T., Yabe, T., Sudoh, M., Satoh, Y., Nakajima, T., Arisawa, M., and Yamada-Okabe, H. (1996). Role of three chitin synthase genes in the growth of *Candida albicans.* J. Bacteriol. **178,** 2416–2419.

Miyazaki, A., and Ootaki, T. (1997). Multiple genes for chitin synthase in the zygomycete fungus *Phycomyces blakesleeanus.* J. Gen. Appl. Microbiol. **43,** 333–340.

Motoyama, T., Fujiwara, M., Kojima, N., Horiuchi, H., Ohta, A., and Takagi, M. (1996). The *Aspergillus nidulans* genes *chsA* and *chsD* encode chitin synthases which have redundant functions in conidia formation. Mol. Gen. Genet. **251,** 442–450.

Motoyama, T., Kojima, N., Horiuchi, H., Ohta, A., and Takagi, M. (1994). Isolation of a chitin synthase gene (*chsC*) of *Aspergillus nidulans.* Biosci. Biotechnol. Biochem. **58,** 2254–2257.

Muller, C., Hjort, C.M., Hansen, K., and Nielsen, J. (2002). Altering the expression of two chitin synthase genes differentially affects the growth and morphology of *Aspergillus oryzae.* Microbiology **148,** 4025–4033.

Munro, C.A., and Gow, N.A. (2001). Chitin synthesis in human pathogenic fungi. Med. Mycol. **39** (suppl. 1), 41–53.

Munro, C.A., Whitton, R.K., Hughes, H.B., Rella, M., Selvaggini, S., and Gow, N.A. (2003). CHS8—A fourth chitin synthase gene of *Candida albicans* contributes to in vitro chitin synthase activity, but is dispensable for growth. Fungal Genet. Biol. **40,** 146–158.

Munro, C.A., Winter, K., Buchan, A., Henry, K., Becker, J.M., Brown, A.J., Bulawa, C.E., and Gow, N.A. (2001). Chs1 of *Candida albicans* is an essential chitin synthase required for synthesis of the septum and for cell integrity. Mol. Microbiol. **39,** 1414–1426.

Nagahashi, S., Sudoh, M., Ono, N., Sawada, R., Yamaguchi, E., Uchida, Y., Mio, T., Takagi, M., Arisawa, M., and Yamada-Okabe, H. (1995). Characterization of chitin synthase 2 of *Saccharomyces cerevisiae.* J. Biol. Chem. **270,** 13961–13967.

Nagata, Y., and Burger, M.M. (1974). Wheat germ agglutinin. Molecular characteristics and specificity for sugar binding. J. Biol. Chem. **249,** 3116–3122.

Nino-Vega, G.A., Carrero, L., and San-Blas, G. (2004). Isolation of the CHS4 gene of *Paracoccidioides brasiliensis* and its accommodation in a new class of chitin synthases. Med. Mycol. **42,** 51–57.

Roncero, C. (2002). The genetic complexity of chitin synthesis in fungi. Curr. Genet. **41,** 367–378.

Ruiz-Herrera, J., Gonzalez-Prieto, J.M., and Ruiz-Medrano, R. (2002). Evolution and phylogenetic relationships of chitin synthases from yeasts and fungi. FEMS Yeast Res. **1,** 247–256.

Schauwecker, F., Wanner, G., and Kahmann, R. (1995). Filament-specific expression of a cellulase gene in the dimorphic fungus *Ustilago maydis.* Biol. Chem. Hoppe Seyler **376,** 617–625.

Schulz, B., Banuett, F., Dahl, M., Schlesinger, R., Schafer, W., Martin, T., Herskowitz, I., and Kahmann, R. (1990). The *b* alleles of *U. maydis*, whose combinations program pathogenic development, code for polypeptides containing a homeodomain-related motif. Cell **60,** 295–306.

Shaw, J.A., Mol, P.C., Bowers, B., Silverman, S.J., Valdivieso, M.H., Duran, A., and Cabib, E. (1991). The function of chitin synthases 2 and 3 in the *Saccharomyces cerevisiae* cell cycle. J. Cell Biol. **114,** 111–123.

Sietsma, J.H., Beth Din, A., Ziv, V., Sjollema, K.A., and Yarden, O. (1996). The localization of chitin synthase in membranous vesicles (chitosomes) in *Neurospora crassa.* Microbiology **142,** 1591–1596.

Specht, C.A., Liu, Y., Robbins, P.W., Bulawa, C.E., Iartchouk, N., Winter, K.R., Riggle, P.J., Rhodes, J.C., Dodge, C.L., Culp, D.W., and Borgia, P.T. (1996). The *chsD* and *chsE* genes of *Aspergillus nidulans* and their roles in chitin synthesis. Fungal Genet. Biol. **20,** 153–167.

Steinberg, G., Schliwa, M., Lehmler, C., Bölker, M., Kahmann, R., and McIntosh, J.R. (1998). Kinesin from the plant pathogenic fungus *Ustilago maydis* is involved in vacuole formation and cytoplasmic migration. J. Cell Sci. **111,** 2235–2246.

Sudbery, P., Gow, N., and Berman, J. (2004). The distinct morphogenic states of *Candida albicans.* Trends Microbiol. **12,** 317–324.

Szabo, Z., Tonnis, M., Kessler, H., and Feldbrugge, M. (2002). Structure-function analysis of lipopeptide pheromones from the plant pathogen *Ustilago maydis.* Mol. Genet. Genomics **268,** 362–370.

Thompson, J.D., Gibson, T.J., Plewniak, F., Jeanmougin, F., and Higgins, D.G. (1997). The CLUSTAL_X windows interface: Flexible strategies for multiple sequence alignment aided by quality analysis tools. Nucleic Acids Res. **25,** 4876–4882.

Wang, Z., Zheng, L., Liu, H., Wang, Q., Hauser, M., Kauffman, S., Becker, J.M., and Szaniszlo, P.J. (2001). WdChs2p, a class I chitin synthase, together with WdChs3p (class III) contributes to virulence in *Wangiella* (*Exophiala*) *dermatitidis.* Infect. Immun. **69,** 7517–7526.

Weber, I., Gruber, C., and Steinberg, G. (2003). A class-V myosin required for mating, hyphal growth, and pathogenicity in the dimorphic plant pathogen *Ustilago maydis.* Plant Cell **15,** 2826–2842.

Wedlich-Söldner, R., Bolker, M., Kahmann, R., and Steinberg, G. (2000). A putative endosomal t-SNARE links exo- and endocytosis in the phytopathogenic fungus *Ustilago maydis.* EMBO J. **19,** 1974–1986.

Weinzierl, G. (2001). Isolierung und Charakterisierung der b-vermittelten Regulationskaskade in *Ustilago maydis.* PhD dissertation (Marburg, Germany: Philipps-Universität).

Xoconostle-Cazares, B., Leon-Ramirez, C., and Ruiz-Herrera, J. (1996). Two chitin synthase genes from *Ustilago maydis.* Microbiology **142,** 377–387.

Xoconostle-Cazares, B., Specht, C.A., Robbins, P.W., Liu, Y., Leon, C., and Ruiz-Herrera, J. (1997). Umchs5,a gene coding for a class IV chitin synthase in *Ustilago maydis.* Fungal Genet. Biol. **22,** 199–208.

Yamada, E., Ichinomiya, M., Ohta, A., and Horiuchi, H. (2005). The class V synthase gene *csmA* is crucial for growth of the *chsA chsC* double mutant in *Aspergillus nidulans.* Biosci. Biotechnol. Biochem. **69,** 87–97.